Cerebral Cortex January 2010;20:141–168
doi:10.1093/cercor/bhp087
Advance Access publication April 30, 2009

Cortical Connections of the Macaque Caudal Ventrolateral Prefrontal Areas 45A and 45B

Marzio Gerbella[1], Abdelouahed Belmalih[1,2], Elena Borra[1], Stefano Rozzi[1] and Giuseppe Luppino[1]

[1]Dipartimento di Neuroscienze, Sezione di Fisiologia, Università di Parma, Istituto Italiano di Tecnologia (IIT, Unità di Parma), I-43100 Parma, Italy

[2]Current address: Institut de Neurosciences Cognitives de la Méditerranée, Marseille Cedex 20, France

We have found that the 2 architectonic subdivisions of the prefrontal area 45, 45A and 45B, display connectivity patterns that clearly distinguish them from one another and from their neighboring architectonic areas. Area 45A is primarily connected to the frontal areas 45B, 12l, caudal 12r, 12o, 10, rostrodorsal 46, 9/8B, 44, 8/FEF (frontal eye field), and the SEF (supplementary eye field), temporal area IPa, and unique among all the studied areas, to the superior temporal polysensory (STP) area and auditory parabelt areas. Area 45B displayed much stronger frontal connections with the oculomotor areas 8/FEF, 8r, and the SEF than those of area 45A, primary connections with areas 12l, caudal 12r, 12o, and 8B, and unlike area 45A, with areas ventrorostral 46, rostral 12r, 12m, and 13m. Temporal connections were all virtually confined to areas IPa, intermediate TEa/m, and TE. Additional labeling was found in lateral intraparietal area. Our data suggest that 45A and 45B are 2 distinct areas, possibly playing a differential role in nonspatial information processing: area 45A corresponds to the prefrontal sector for which a role in communication behavior and homology with the human area 45 was proposed, whereas area 45B is a distinct prearcuate area, possibly affiliated to the oculomotor frontal system.

Keywords: area STP, auditory cortex, inferotemporal cortex, frontal lobe, prefrontal cortex

Introduction

The caudal part of the ventrolateral prefrontal cortex (VLPF) of the macaque, bordered dorsally by the principal sulcus (PS), caudally by the inferior arcuate sulcus (IAS), and rostrally by the infraprincipal dimple (IPD), is a part of at least 3 functionally distinct regions. A caudal one, close and within the arcuate sulcus, includes the frontal eye field (FEF) and is involved in oculomotor functions (Bruce et al. 1985). A dorsal one, close and within the PS, has been considered to play a role in visuospatial information processing (see, e.g., Levy and Goldman-Rakic 2000). Finally, a more ventral sector is involved in higher-order processing of nonspatial information (Levy and Goldman-Rakic 2000; Passingham et al. 2000; Romanski 2004).

According to Petrides and Pandya (1994, 2002), this last caudal VLPF sector corresponds to an architectonic area, area 45, formed by 2, slightly different, architectonic subdivisions: a caudal one, 45B, lying ventrally in the prearcuate bank and a rostral one, 45A, extending on the rostrally adjacent inferior frontal convexity, as far as the IPD. Petrides and Pandya (2002) also showed that area 45, as a whole, is connected to several cortical areas, including auditory-related areas of the superior temporal gyrus (STG) and the multimodal area superior temporal polysensory (STP) of the upper bank of the superior temporal sulcus (STS). Based on these data and on some comparative cytoarchitectonic criteria, they proposed that area 45 is the possible homolog of the corresponding language-related area of the human brain.

However, the subdivision of the caudal VLPF proposed by Petrides and Pandya (1994, 2002) markedly differs, from the other proposed subdivisions. Specifically 1) the sector 45B, located ventral to the FEF, as architectonically and/or functionally defined (Huerta et al. 1987, Stanton et al. 1989) and mostly corresponding to areas Frontal Ventral (FV) identified by Huerta et al. (1987) or FDi identified by Stanton et al. (1993), has been included along with the ventral part of the FEF, within a single inferior prearcuate area in most of the other architectonic studies (Walker 1940; Barbas and Pandya 1989; Preuss and Goldman-Rakic 1991); (2) the sector 45A occupies a cortical sector of a highly controversial architectonic attribution, assigned to areas 46 and 12 by Walker (1940), to areas 8 ventral and 46 by Barbas and Pandya (1989) and mostly to area 12 by Preuss and Goldman-Rakic (1991) and Romanski (2004, 2007). These differences are the source of conflicting interpretations on the attribution of functional and connectional data to specific areas. For example, within and just caudal to the IPD, there are neurons involved in the control of communicative behavior (Romanski et al. 2005, Sugihara et al. 2006), which is in line with the proposed homology between the monkey and the human area 45. However, according to Romanski (2004, 2007), this sector is a part of area 12, and not area 45.

In a recent multiarchitectonic study (Gerbella et al. 2007), we recognized robust multimodal criteria for considering the 2 area 45 sectors, 45B and 45A, architectonically distinct from one another and from their neighboring VLPF areas. Furthermore, indirect evidence showed that STG auditory-related areas and area STP appear to project, in the caudal VLPF, only in the location of 45A (Petrides and Pandya 1988; Seltzer and Pandya 1989; Romanski, Tian, et al. 1999; Saleem et al. 2008; Munoz et al. 2009). These data suggest that area 45A is 1) connectionally distinct from 45B, and 2) a distinct cortical entity and not a part of areas 46, 12, or 8.

In the present study, we used architectonic data to guide the location of tracer injections to assess whether 1) the connectivity patterns of areas 45A and 45B differ from one another and from the neighboring areas 12, 46, 8r, and 8/FEF, and 2) the area 45A is the selective VLPF target of afferents from the STG and area STP. These data have been partially presented in the abstract form (Luppino et al. 2008).

Methods

Subjects and Surgical Procedures

The experiments were carried out in 7 macaque monkeys (3 *Macaca fascicularis*, 2 *Macaca nemestrina*, and 2 *Macaca mulatta*), in which the neural tracers were injected in the architectonic areas 45A, 45B,

8/FEF, 8r, 46, and 12. The animal handling as well as surgical and experimental procedures complied with the European guidelines (86/609/EEC and 2003/65/EC Directives) and Italian laws in force on the care and use of laboratory animals, and were approved by the Veterinarian Animal Care and Use Committee of the University of Parma and authorized by the Italian Health Ministry.

Under general anesthesia and aseptic conditions, each animal was placed in a stereotaxic apparatus, and an incision was made in the scalp. The skull was trephined to remove the bone overlying the target region and the dura was opened to expose the caudal VLPF. After the tracer injections, the dural flap was sutured, the bone was replaced, and the superficial tissues were sutured in layers. During surgery, hydration was maintained with saline and temperature was maintained using a heating pad. Heart rate, blood pressure, respiratory depth, and body temperature were continuously monitored. Upon recovery from anesthesia, the animals were returned to their home cages and closely monitored. Dexamethasone and prophylactic broad-spectrum antibiotics were administered pre- and postoperatively. Furthermore, analgesics were administered intra- and postoperatively.

Selection of the Injection Sites

The choice of the injection sites was based on the identification of anatomical landmarks (e.g., the arcuate sulcus, the PS, and the IPD, when present) and using, as frame of reference, an average architectonic map of the caudal VLPF providing an estimate of the average location of areas 45A, 45B, 8/FEF, and 8r, with respect to the IAS, PS, and IPD (Gerbella et al. 2007).

In cases 36 (left and right hemisphere) and 37 (left hemisphere), the choice of the injection sites in the prearcuate area 8/FEF was also guided by the intracortical microstimulation (ICMS) data, using procedures similar to those of some earlier connectional studies (e.g., Huerta et al. 1987; Stanton et al. 1988; Schall et al. 1995). For this purpose, the ventral prearcuate bank was explored with microelectrode (1–1.5 MΩ at 1000 KHz) penetrations spaced at about 1-mm intervals. Locations of the microelectrode penetrations were marked on a photographic print of the exposed cortex, using the blood vessel patterns as frame of reference. In each penetration, the electrode was inserted into the cortex at a distance of about 1–1.5 mm from the sulcus and advanced for at least 5–6 mm through the bank, whereas recording single and/or multiunit activity, indicative of cortical grey matter. Along the penetrations, at approximately 1-mm intervals, trains of cathodal current (0.2-ms pulse duration, 300-Hz frequency, train duration of 50–100 ms) were delivered at current intensities <100 μA. The occurrence of saccadic eye movements evoked by the electrical stimulation was assessed by direct visual inspection by at least 3 researchers.

Tracer Injections and Histological Procedures

Once the appropriate site was chosen, the retrograde tracers Fast Blue (FB, 3% in distilled water, Dr Illing Plastics GmbH, Breuberg, Germany), Diamidino Yellow (DY, 2% in 0.2 M phosphate buffer at pH 7.2, Dr Illing Plastics) and Cholera Toxin B subunit, conjugated with Alexa 488 (CTB green, CTBg) or Alexa 594 (CTB red, CTBr, 1% in phosphate-buffered saline [PBS], Invitrogen–Molecular Probes, Eugene, OR), the mostly anterograde tracer—biotinylated dextran amine (10 000 MW, BDA, 10% 0.1 M phosphate buffer, pH 7.4; Invitrogen–Molecular Probes), and the retro-anterograde tracer-Dextran conjugated with tetramethylrhodamine (10 000 MW, Fluoro-Ruby, FR, 10% 0.1 M phosphate buffer, pH 7.4; Invitrogen–Molecular Probes), were slowly pressure-injected through a glass micropipette (tip diameter: 50–100 μm) attached to a 1- or 5-μL Hamilton microsyringe (Reno, NV) at about 1.2–1.5 mm below the cortical surface in the inferior frontal convexity, or at different depths in the ventral prearcuate bank. Table 1 summarizes the locations of injections, the injected tracers, and their amounts.

After appropriate survival periods following the injections (28 days for BDA and FR, 12–14 days for FB, DY, and CTB), each animal was deeply anesthetized with an overdose of sodium thiopental and perfused consecutively with saline, 3.5–4% paraformaldehyde, and 5% glycerol, prepared in 0.1 M phosphate buffer and pH 7.4, through the left cardiac ventricle. Each brain was then blocked coronally on a stereotaxic apparatus, removed from the skull, photographed, and placed in 10% buffered glycerol for 3 days and 20% buffered glycerol for 4 days. Finally, it was cut frozen into coronal sections of 60-μm thickness.

Table 1
Monkeys species, localization of the cortical injections and tracers employed in the experiments

Monkey	Species	Hemisphere	Area	Tracer	Amount
Case 23	*Macaca fascicularis*	L	46v	FB 3%	2 × 0.2 μL
Case 26	*Macaca nemestrina*	L	45B	DY 2%	1 × 0.2 μL
		L	46v	CTBg 1%	1 × 1 μL
		L	12	FB 3%	1 × 0.2 μL
Case 30	*Macaca nemestrina*	R	45B	FB 3%	1 × 0.2 μL
Case 35	*Macaca mulatta*	R	8/FEF	FR 10%	1 × 1 μL
Case 36	*Macaca fascicularis*	L	8/FEF	DY 2%	1 × 0.2 μL
		L	45B	FB 3%	1 × 0.2 μL
		L	45A	CTBg 1%	1 × 1 μL
		R	8/FEF	FR 10%	1 × 1 μL
		R	45B	BDA 10%	1 × 1 μL
Case 37	*Macaca mulatta*	L	8/FEF	CTBg 1%	1 × 1 μL
		L	8r	CTBr 1%	1 × 1 μL
		L	45A	FB 3%	2 × 0.2 μL
		R	45A	BDA 10%	1 × 1 μL
		R	45B	FR 10%	1 × 1 μL
Case 39	*Macaca fascicularis*	L	45A	FR 10%	2 × 1 μL
		R	8r	FB 3%	1 × 0.2 μL
		R	12	DY 2%	1 × 0.2 μL

In all the cases in which FB, DY, or CTB were injected, every fifth section was mounted, air-dried, and quickly coverslipped for fluorescence microscopy. In Cases 36r and 37r, one series of each fifth section was processed for the visualization of BDA (incubation 60 h), using a Vectastain ABC kit (Vector Laboratories, Burlingame, CA) and 3,3′-diaminobenzidine (DAB) as a chromogen. The reaction product was intensified with cobalt chloride and nickel ammonium sulfate. In Cases 36r and 37r in which BDA was injected in other caudal VLPF areas, one series of each fifth section was processed for the visualization of FR and BDA using a double-labeling protocol very similar to that described by Morecraft et al. (2001). To obtain comparable results, the same protocol was used in Cases 35r and 39l. In this procedure, sections from Cases 36r and 37r were first processed for the visualization of BDA as described earlier, except for a shorter incubation period in the ABC solution (overnight) and that BDA was stained brown using DAB. After rinsing in PBS, the sections were incubated in avidin–biotin blocking reagent (Vector SP-2001) and rinsed again in PBS. Subsequently, these sections and those from Cases 35r and 39l were incubated for 72 h at 4 °C in a primary antibody solution of rabbit anti-FR (1:3000; Invitrogen) in 0.3% Triton, 5% normal goat serum in PBS, and, after rinsing in PBS, were incubated in biotinylated secondary antibody (1:200, Vector) in 0.3% Triton, 5% normal goat serum in PBS. Subsequently, after rinsing in PBS, FR labeling was visualized using the Vectastain ABC kit (Vector Laboratories, Burlingame, CA) and the Vector SG peroxidase substrate kit (SK-4700, Vector) as a chromogen. In this way, BDA labeling was stained brown and the FR labeling was stained blue in the same tissue sections. In additional sections, for a more clear definition of the FR injection sites (refer below), we used a different, less sensitive, protocol. The sections were washed in 0.3% Triton in 0.05 M Tris-buffered saline of pH 7.6 (TBST), incubated in a ready-to-use Peroxidase blocking kit solution (Chemicon International, Temecula, CA), rinsed again in TBST, and placed in a solution of rabbit anti-FR (1:3000, Invitrogen) TBST for 72 h at 4 °C. After rinsing in TBST, the sections were placed in a ready-to-use anti-rabbit Poly-HRP IHC Detection Kit (Chemicon International) solution, rinsed again, and the FR labeling was finally visualized using DAB as a chromogen.

In Case 36 (left and right hemisphere), one series of each tenth section was immunoreacted for the visualization of the mouse monoclonal antibody SMI-32 immunoreactivity (originally provided by Sternberger Monoclonals, Baltimore, MD, now provided by Covance, Princeton, NJ, Cat. N° SMI-32R), as described by Gerbella et al. (2007). In all the cases, one series of each fifth section was stained by Nissl method (0.1% thionin in 0.1 M acetate buffer, pH 3.7).

Data Analysis

Injection Sites and Distribution of Retrogradely Labeled Neurons

The criteria used for the definition of the injection sites and the identification of FB, DY, CTBg, CTBr, and BDA labeling have been

described in earlier studies (Luppino et al. 2001, 2003; Rozzi et al. 2006). The FR injection site, in sections stained with the ABC-based protocol, was defined by a very heavily stained area surrounding the point of tracer administration, of about 1 mm in diameter for injections of 1 μL, which was only slightly larger than the injection site defined in the control experiments in fluorescence microscopy. However, in all the cases the injection site was surrounded by a region of dense, nonspecific-cell and background staining that, though with a decrease in intensity, extended for several millimeters, invading Case 37r (injection in area 45B) area 45A and Case 39l (injection in area 45A) areas 45B and 8r. In sections stained with the poly-HRP–based protocol, the size of the heavily stained area corresponding to the injection site was very similar, but the intensity of the surrounding nonspecific staining was much lower and more restricted. These sections were, therefore, used for a more precise definition of the fringe of the injection site, considered, as in other studies (e.g., Morecraft et al. 2007), as the region where the dense precipitate diminished and the fibers emanating from the injection site and neuron profiles were clearly distinguishable. In spite of this problem, we adopted the ABC-based protocol for describing the connectivity patterns observed following FR injections, because of its very high sensitivity in the visualization of retrograde labeling, and even higher sensitivity in the visualization of the anterograde labeling.

The injection sites were attributed to the architectonic areas of the caudal VLPF with the analysis of adjacent Nissl-stained sections. The location of the injection sites and cytoarchitectonic borders was then reported on a 2-dimensional (2D) reconstruction of the injected hemisphere.

The distribution of retrograde (for all tracer injections, but BDA) and anterograde (for BDA and FR injections) labeling was analyzed in sections every 300 μm and plotted in sections every 600 μm, together with the outer and inner cortical borders, using a computer-based charting system. Following injections of BDA, given the relative paucity of retrograde labeling, only anterogradely labeled terminals were plotted. The distribution of the labeling in the PS, STS, and lateral bank of the intraparietal sulcus (IPS) was visualized in 2D reconstructions obtained using the same software, as follows (for more details, see Matelli et al. 1998). In each plotted section, the cortical region of interest was subdivided into columnar bins by lines perpendicular to the cortical surface, connecting the outer and inner cortical contours. The cortex was then unfolded at the level of a virtual line connecting the midpoints of all the perpendicular lines, approximately positioned at the border between layers III and IV. The unfolded sections were then aligned and the labeling was distributed along the space between the 2 consecutive plotted sections (600 μm). Sections through the PS were aligned to correspond with the fundus, those through the STS were aligned to correspond with the fundus and the middle of the floor, and those through the lateral bank of the IPS were aligned to correspond with the lateral lip of the sulcus. Data from individual sections were also imported into the 3-dimensional (3D) reconstruction software (Bettio et al. 2001) providing volumetric reconstructions of the monkey brain, including connectional and architectonic data. The labeling distribution on the exposed cortical surfaces was visualized in the dorsolateral, mesial, and bottom views of the 3D reconstructions of the hemispheres.

Areal Attribution of the Labeling

The attribution of the labeling to the caudal VLPF areas was made according to the cytoarchitectonic criteria described by Gerbella et al. (2007). The criteria and maps adopted for the areal attribution of the labeling observed in other cortical regions were mostly similar to those adopted in previous studies (Rozzi et al. 2006; Borra et al. 2008). In the frontal lobe, the orbitofrontal cortex and the gyral convexity cortex rostral to area 45A were subdivided according to Carmichael and Price (1994), except for the rostral border of area 45A with area 12r, set at the level of the IPD, as described by Petrides and Pandya (1994, 2002) and Gerbella et al. (2007). The dorsolateral prefrontal cortex (DLPF) was subdivided according to Petrides and Pandya (1994, 1999, 2002), except for the periprincipal area 46, considered as a single entity because of the difficulty in defining the subdivisions defined by these authors. The distribution of the labeling in this area was described in terms of its dorsal or ventral location with respect to the fundus of the PS (46d and 46v, respectively), and rostral or caudal location within each of these 2 sectors. The inferotemporal convexity cortex and the STS were subdivided according to Saleem and Tanaka (1996) and Boussaoud et al. (1990), respectively, and the STG and auditory belt areas were subdivided according to Kaas and Hackett (2000; see also Saleem et al. 2008). In the inferior parietal lobule (IPL), the gyral convexity areas were defined according to Gregoriou et al. (2006), and those of the lateral bank of the IPS were defined according to the functional and connectional criteria described by Borra et al. (2008).

Quantitative Analysis and Laminar Distribution of the Labeling

In all the cases of retrograde tracer injections, except for Cases 37r FR and 39l FR (invasion of nonspecific staining in neighboring areas), we counted the number of labeled neurons plotted in the ipsilateral hemisphere in sections every 600-μm intervals, beyond the limits of the injected area. Cortical afferents to the studied caudal VLPF areas were then expressed in terms of the percent of labeled neurons found in a given cortical subdivision, with respect to the overall labeling.

Finally, to obtain information on the organization of the laminar patterns of the observed connections, the labeling attributed to a given area and reliably observed across different sections and cases was analyzed in sections every 300 μm in terms of the following: 1) laminar distribution of the anterogradely labeled terminals (for BDA and FR injections) and 2) percent of retrogradely labeled neurons located in the superficial (II–III) versus deep (V–VI) layers. These data were then interpreted, when possible, according to the criteria used by Felleman and Van Essen (1991) in their functional hierarchical model of cortical connections.

Results

Injection Sites

All the injection sites presented in this study, most of them illustrated in Figures 1–4, were completely restricted to the cortical grey matter, involving the entire cortical thickness or at least the middle cortical layers, except for the CTBg injection in Case 36l, mostly limited to layers II and III.

In area 45A, the injection sites were entirely located within its architectonic borders, in the mid-caudal (Cases 37r BDA, Fig. 1*A* and 39l FR, Fig. 1*B*), mid-rostral (Case 37l FB, Fig. 1*C*), or rostral (Case 36l CTBg, Fig. 1*D*) parts, together involving a large extent of it. Figure 2*A1* and *B1* shows the rostral FB injection site of Case 37l and the CTBg injection site of Case 36l, respectively, placed rostrally in area 45A, where an increase in cell size from the upper to the lower part of layer III was evident (Fig. 2*A2* and *B2*). This evident layer III size gradient was a major architectonic feature used for attributing injection sites to area 45A or to the rostrally adjacent area 12r, where layer III is denser and rather homogeneous in cell size and density (Fig. 2*A3* and *B3*).

In area 45B, tracer injections were placed at different depths and dorsoventral levels of the prearcuate bank, together involving almost its entire extent. In Case 30r (Fig. 1*F*), though the FB injection halo marginally involved the transitional zone with the dorsally adjacent area 8/FEF, the injection core and most of the halo were located within the limits of area 45B (Fig. 3*A1* and *A2*), characterized by 1) large, deeply stained pyramids in the lowest layer III, standing out against an overall layer III cell population, relatively homogeneous in size and density; and 2) a cell sparse layer V, not clearly sublaminated, and all populated virtually by small pyramids. In Cases 36l FB (Fig. 1*D*) and 36r BDA (Fig. 1*E*), the tracer injections were placed in the ventralmost and the middle part of area 45B, respectively, as architectonically defined (Fig. 3*B1* and *B2* and

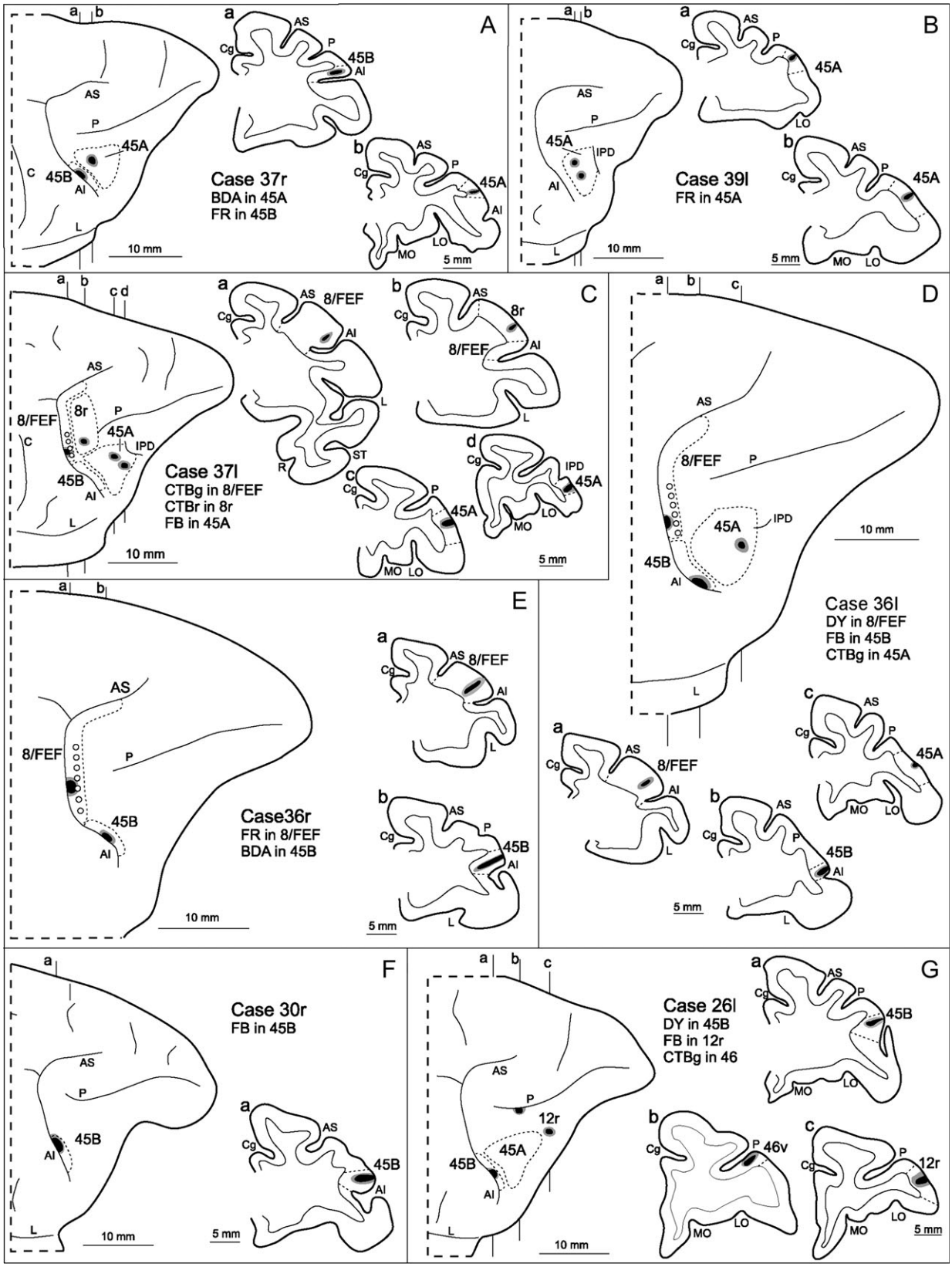

Figure 1. Location of injection sites in Cases 37r (A), 39l (B), 37l (C), 36l (D), 36r (E), 30r (F), and 26l (G), shown on dorsolateral views of the injected hemispheres and in coronal sections through the core (shown in black) and the halo (shown in lighter gray). Dashed lines on the drawings of the hemispheres and of the sections mark the cytoarchitectonic borders of the injected areas. Empty circles on the prearcuate cortex of Cases 37l (*C*), 36l (*D*), and 36r (*E*) mark the insertion points of electrode penetrations from which eye movements were evoked with ICMS (current intensity <50 μA). For the sake of comparison, all the reconstructions in this and in the subsequent figures are shown as a right hemisphere. AI = inferior arcuate sulcus; AS = superior arcuate sulcus; C = central sulcus; Cg = cingulate sulcus; L = lateral fissure; LO = lateral orbital sulcus; MO = medial orbital sulcus; P = principal sulcus; R = rhinal fissure; ST = superior temporal sulcus.

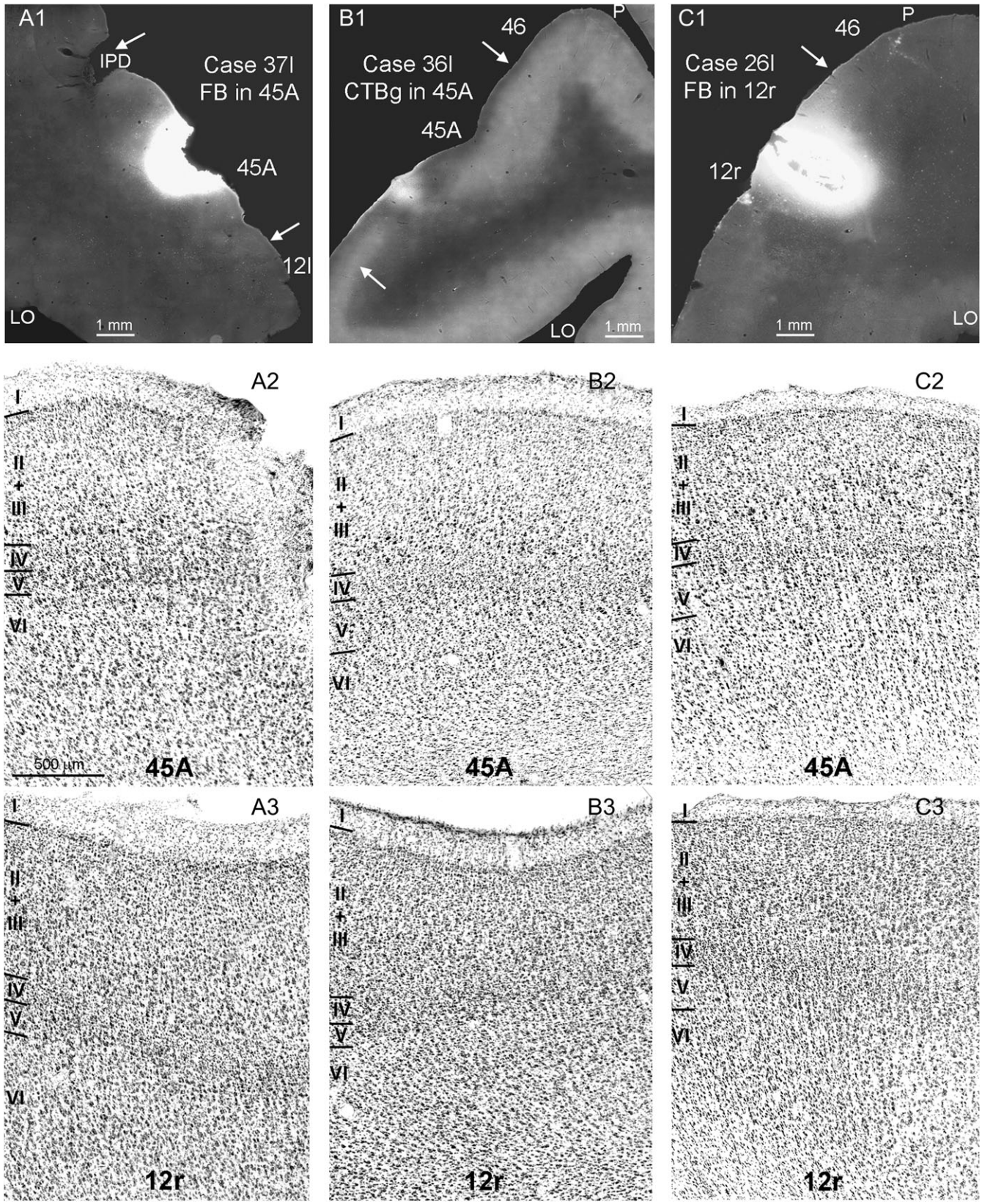

Figure 2. Injections sites in areas 45A and 12r and major cytoarchitectonic features used for their areal attribution. Upper row: low-power photomicrographs showing, in *A1* and *B1*, the injection sites in area 45A of Cases 37l FB and 36l CTBg, respectively, and, in *C1*, the injection site in area 12r of Case 26l FB; arrows mark the borders of the injected area. Middle row: photomicrographs of Nissl-stained sections through area 45A from Cases 37l (*A2*), 36l (*B2*), and 26l (*C2*) showing the evident increase in cell size from the upper to the lower part of layer III, which is a distinguishing architectonic feature of area 45A; the fields in *A2* and *B2* were taken from sections adjacent to those in *A1* and *B1*, respectively. Lower row: photomicrographs of Nissl-stained sections through area 12r from Cases 37l (*A3*), 36l (*B3*), and 26l (*C3*) showing a cell-dense, rather homogeneous layer III, which distinguish this area from area 45A; the field in *C3* was taken from a section adjacent to that in *C1*. Calibration bar, shown in *A2*, applies to *A2-C3*. Abbreviations as in Figure 1.

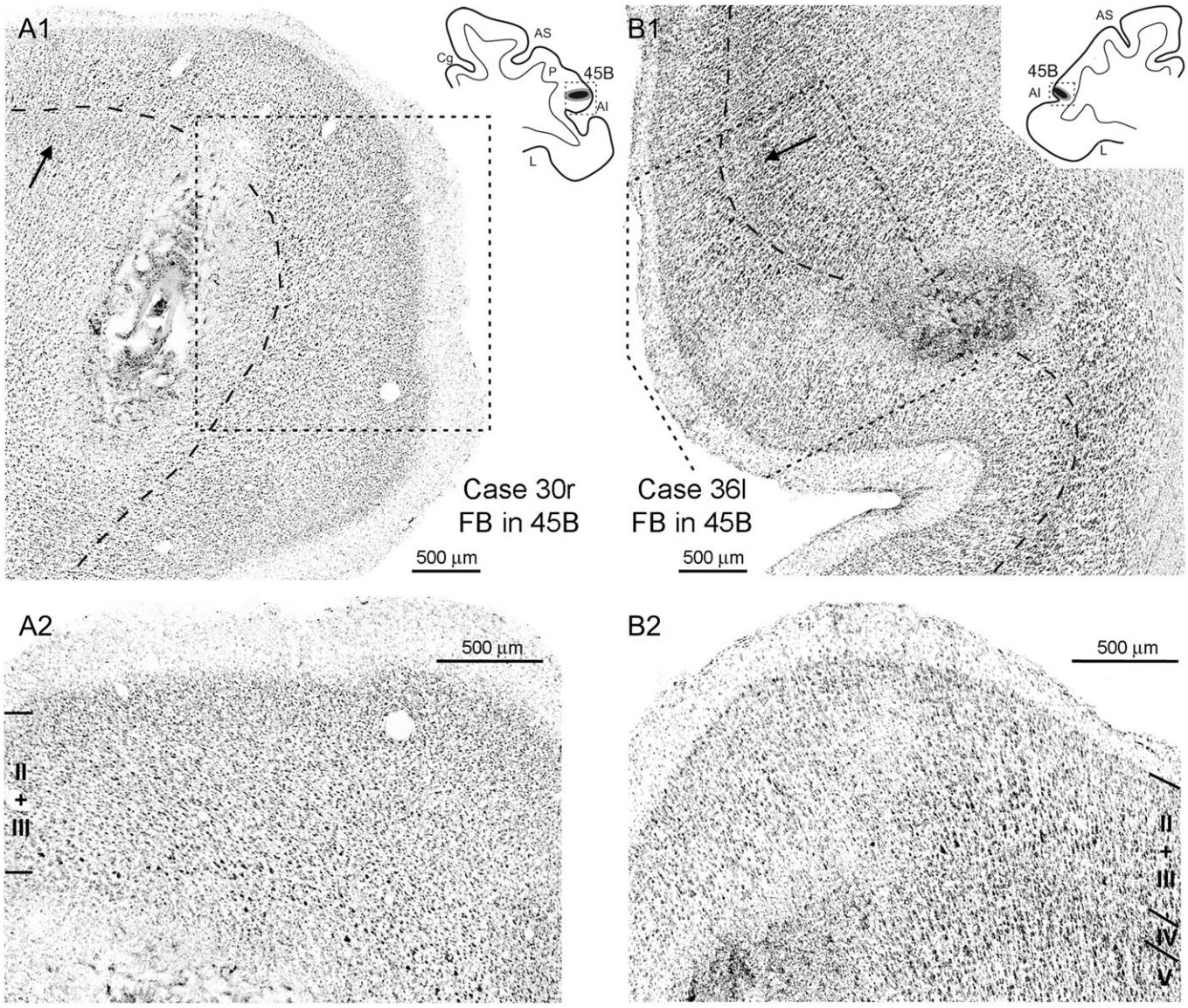

Figure 3. Injections sites in area 45B and major cytoarchitectonic features used for their areal attribution. In *A1* and *B1* low-power photomicrographs of Nissl-stained sections show the injection sites in area 45B of Cases 30r FB and 36l FB, respectively; dashed boxes on the section drawings indicate the locations of the photomicrographs; in each photomicrograph, the dashed line marks the border between layer III and layer IV and the arrow marks the cytoarchitectonic border with area 8r (*A1*) or 45A (*B1*). A2 and B2: higher magnification views of the fields indicated by dashed boxes in *A1* and *B1*, respectively, showing the presence, close to the injection sites, of large pyramids in the lowest part of layer III, which are a distinguishing architectonic feature of area 45B. Abbreviations as in Figure 1.

Fig. 4*A1-A3*). In both these hemispheres, SMI-32 immunostained sections, through the injection site (Fig. 4*A4*), displayed large, lowest layer III immunopositive pyramids and a poorly immunoreactive layer V, which are the 2 distinguishing chemoarchitectonic features of area 45B (Gerbella et al. 2007). In Cases 26l DY (Fig. 1*G*) and 37r FR (Fig. 1*A*), tracer injections involved the mid-ventral and mid-dorsal parts of area 45B, respectively.

In area 8/FEF, tracer injections in Cases 36l (DY, Fig. 1*D*), 36r (FR, Fig. 1*E*), and 37l (CTBg, Fig. 1*C*) were placed in its ventral part, based on ICMS data. In Case 35r, the FR injection was placed more dorsally in the prearcuate bank, at a medio-lateral level corresponding to the caudal tip of the PS. As observed in other studies (e.g., Huerta et al. 1987; Stanton et al. 1988; Schall et al. 1995), the saccades could be easily and reliably detected more dorsally in the FEF with current intensities <50 μA, whereas they progressively reduced in amplitude more ventrally, and in the ventralmost penetrations hosting responsive sites they were much less reliably detected. In several cases, increasing the stimulus train duration (100 ms) improved the detection of these small saccades. In the ventralmost part of the prearcuate bank, ICMS was never effective in eliciting eye movements with current intensities <50 μA, even with 100-ms stimulus train duration. In Cases 36l DY, 36r FR, and 37l CTBg, the tracer injections were all placed corresponding to the of ICMS responsive sites (see, e.g., Fig. 4*B1*). These injections, as well as the electrode penetrations hosting responsive sites (circles in Fig. 1*C–E*) were all located within the architectonic area 8/FEF (see, e.g., Fig. 4*B2* and *B3*), where large layer V pyramids were very much evident in the SMI-32 immunostained material also (Fig. 4*B4*). In contrast, those penetrations

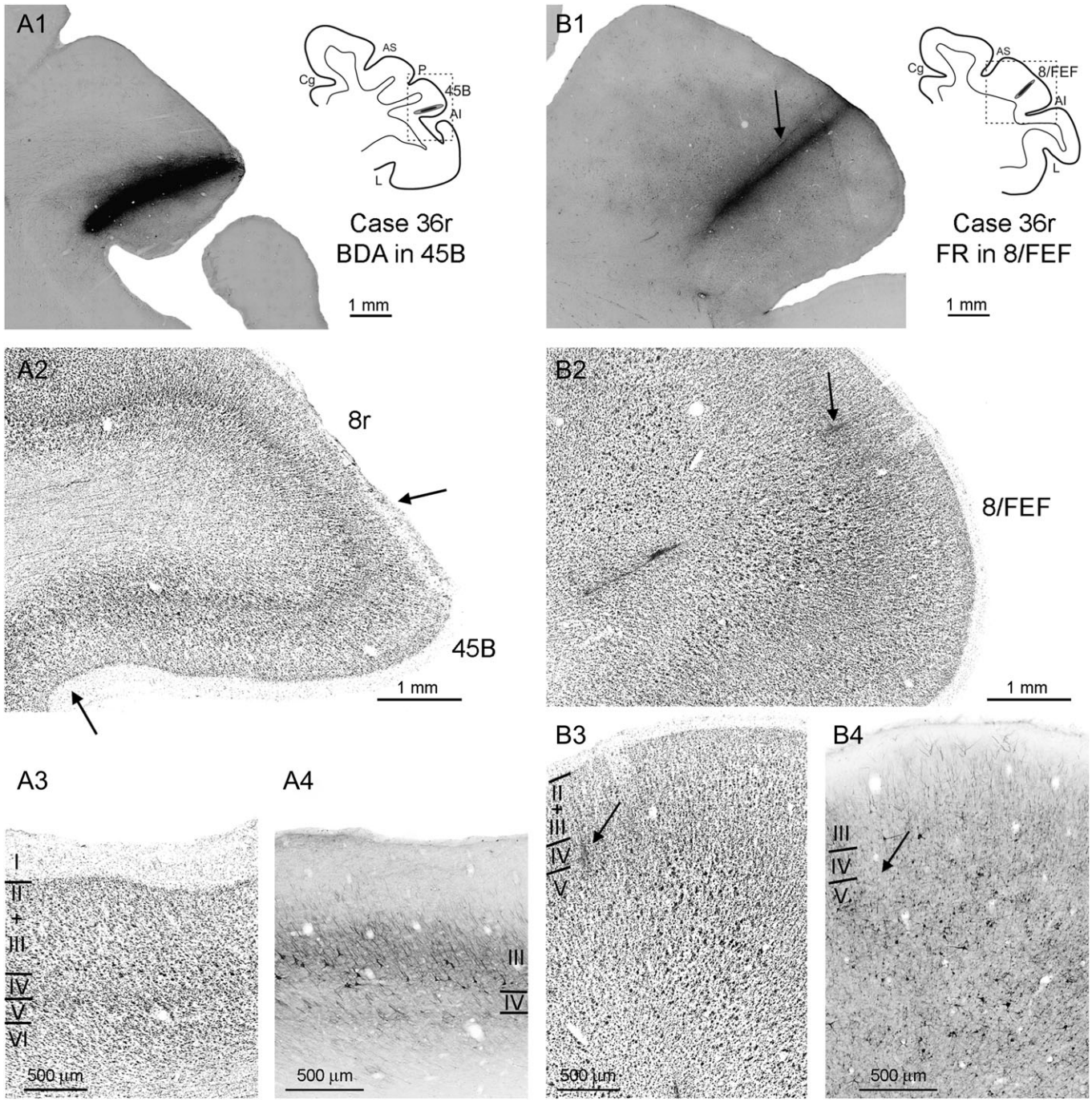

Figure 4. Injections sites in Case 36r and major architectonic features used for their areal attribution. (*A1* and *B1*) Low-power photomicrographs of the BDA (*A1*) and the FR (*B1*) injection sites, placed in areas 45B and 8/FEF, respectively; dashed boxes on the section drawings indicate the locations of the photomicrographs. (*A2* and *B2*) Low-power photomicrographs of Nissl-stained sections adjacent to the sections shown in (*A1*) and (*B1*), respectively; arrows in *A2* mark the border of area 45B. (*A3* and *B3*) higher magnification views of fields taken from the Nissl-stained sections shown in *A2* and *B2*, respectively, showing the presence of large, lowest layer III pyramids in area 45B and of large layer V pyramids in area 8/FEF. (*A4* and *B4*) Higher magnification views of the same fields shown in A3 and B3, respectively, taken from adjacent SMI-32 immunoreacted sections, showing the presence of large layer III immunopositive pyramids in area 45B and of large immunopositive layer V pyramids in area 8/FEF. Arrows in *B1-B4*, mark the track of an electrode penetration in which ICMS was effective in evoking eye movements with current intensities <50 μA. Abbreviations as in Figure 1.

in which ICMS was not effective in eliciting eye movements were all located in the architectonic area 45B. This observation is in very good agreement with the study by Stanton et al. (1989), who demonstrated that the prearcuate sector hosting large layer V pyramids corresponds to the FEF, as functionally defined in the awake macaques.

In areas 8r, 46, and 12r, the injection sites were mostly placed close to areas 45B and/or 45A. In area 8r, a newly defined architectonic area located caudally in the prearcuate convexity cortex (Gerbella et al. 2007), the tracer injections involved its ventral (Case 37l CTBr, Fig. 1*C*) or midventral part (Case 39r FB). In area 46, the injections (Case 26l CTBg, Fig. 1*G*,

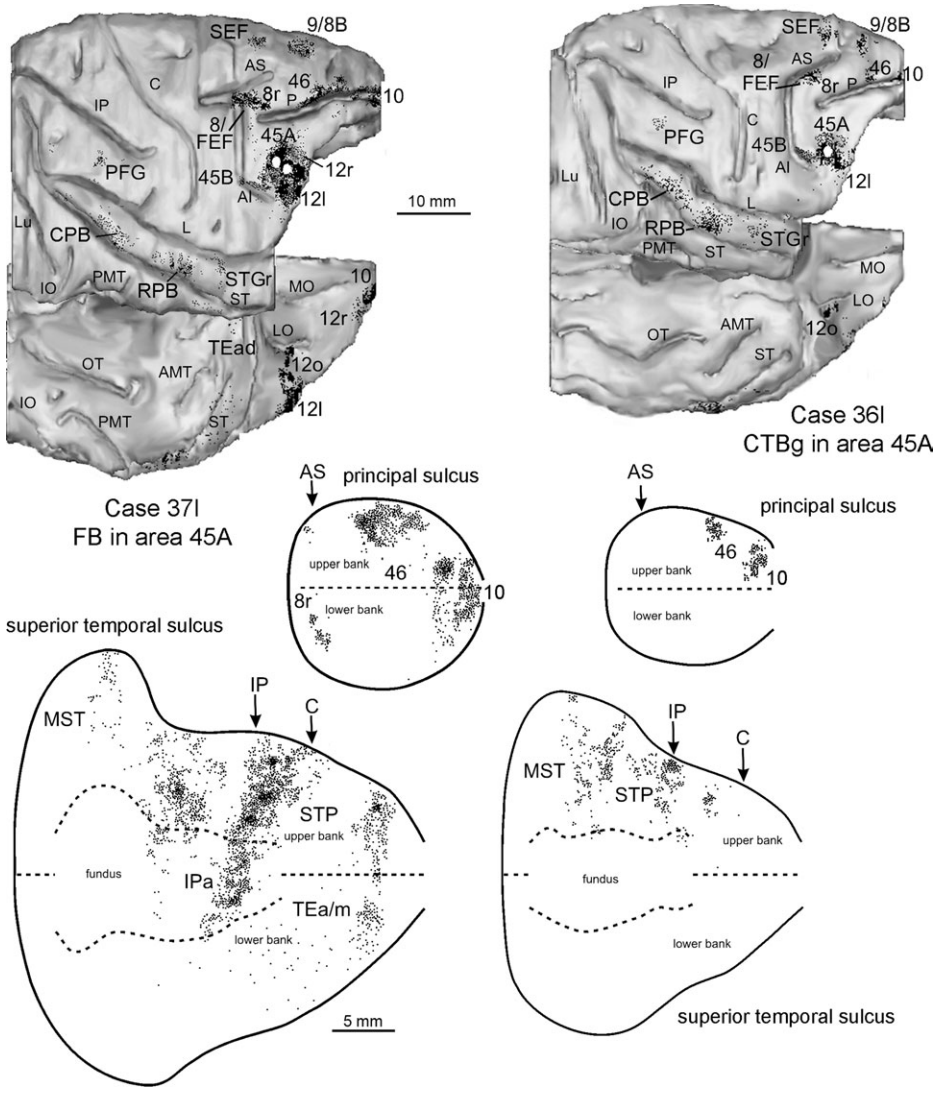

Figure 5. Distribution of the retrograde labeling observed following injections in area 45A in Cases 37l (FB) and 36l (CTBg), shown in dorsolateral and bottom views of the 3D reconstructions of the injected hemispheres (upper part) and in 2D reconstructions of the PS and of the STS (lower part). Each dot corresponds to one labeled neuron. Each 2D reconstruction of the PS was aligned to correspond with the fundus. The dashed line indicates the fundus and the continuous lines the lips of the sulcus. The arrow marks the rostralmost level of the superior arcuate sulcus (AS). Each 2D reconstruction of the STS was aligned to correspond with the fundus and middle of the floor. The dashed lines indicate the fundus and the upper and lower edges of the floor, the continuous lines the lips of the sulcus. Arrows mark the rostralmost level of the IPS (IP) and of the central sulcus (*C*). The location of each tracer injection, is shown as a white area on the dorsolateral view of the hemisphere. AMT = anterior middle temporal sulcus; IO = inferior occipital sulcus; Lu = lunate sulcus; OT = occipitotemporal sulcus; PMT = posterior middle temporal sulcus. Other abbreviations as in Figure 1.

and Case 23l FB) involved its caudoventral part, which is chemoarchitectonically different from its more rostral part (Gerbella et al. 2007) and may correspond, at least in part, with the architectonic area 9/46v defined by Petrides and Pandya (1994, 2002). In area 12r, tracer injections (Case 26l FB, Fig. 1*G* and Case 39r DY) were placed in its caudal part. Figure 2*C1* shows the FB injection site of Case 26l, placed in the caudalmost part of area 12r, characterized by a layer III that is rather dense and homogeneous in cell size and density (Fig. 2*C3*), in the vicinity of area 45A (Fig. 2*C2*).

In general, tracer injections placed in different parts of each caudal VPLF area or field yielded quite consistent distributions and patterns of labeling across different cases and animals. Quantitative analysis showed, with few exceptions, similar percent distributions of the labeling. Injections of retro-anterograde (FR) or predominantly anterograde (BDA) tracers in areas 45A, 45B, and 8/FEF showed that virtually all the cortical connections of these areas were reciprocal.

Connections of Area 45A

Figures 5–7 show the distribution of the retrograde labeling observed in Cases 37l FB and 36l CTBg, and the anterograde labeling observed in Case 37r BDA. The distribution of the retrograde and anterograde labeling in Case 39l FR (not shown) was comparable with these cases. Retrograde labeling in Cases 37l and 36l was remarkably similar (Table 2), although there were many fewer labeled cells that resulted from the tracer injection in Case 36l, possibly because the injection site did not extend to deeper cortical layers.

In the prefrontal cortex (Fig. 5), the labeling was very dense in the adjacent areas 45B, 12l, and area 12r, where the labeling

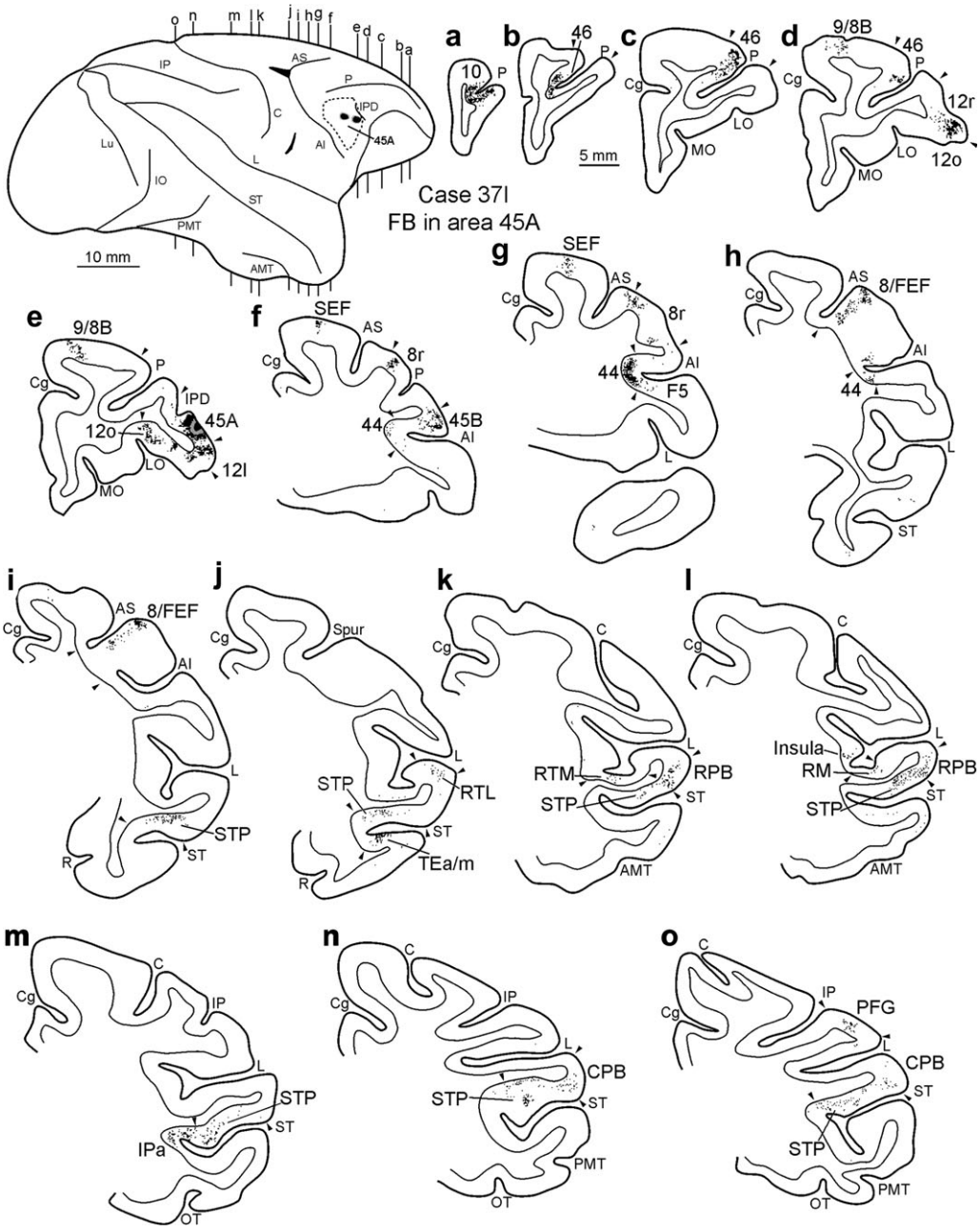

Figure 6. Distribution of the retrograde labeling observed in Case 37l FB, shown in drawings of coronal sections. Sections are shown in a rostral to caudal order (a–o). Arrowheads indicate borders between different areas. The dorsolateral view of the injected hemisphere in the upper left part of the figure shows the levels at which the sections were taken, the border of area 45A and the location of the injection sites. Conventions and abbreviations as in Figures 1 and 5.

was: limited to its caudal half (12r caudal in Table 2; Fig. 6, sections d–f, and Fig. 7, sections c–f), very weak in area 8r (Fig. 6, sections f and g, and Fig. 7, section f), and almost absent in the ventrocaudal part of area 46. Area 8/FEF was also densely labeled: marked cells were mostly located in its dorsal part, where the labeled terminals observed in Case 37r were more concentrated (Fig. 6, sections h and i, and Fig. 7, section g). Relatively dense connections were also found with the DLPF areas 8B, caudalmost 9 (Fig. 6, sections d and e, and, Fig. 7, section d), and the rostral part of dorsal area 46 (Fig. 6, sections b–d, and Fig. 7, sections b–d) and area 10 (Fig. 6, section a, and Fig. 7, section a). There was dense label in the fundus of the rostral part of the PS and weak label in the ventral bank in Case 37l that was not found in Case 36l CTBg. In the orbitofrontal cortex, dense connections were observed with area 12o (Fig. 6, section e, and Fig. 7, sections d and e). Two other frontal sectors were labeled, with some variability across the cases: one, dorsorostrally in the dorsal premotor cortex (Fig. 6, sections f and g, and Fig. 7, sections e and f), which corresponded to the supplementary eye field (SEF; Schlag and Schlag-Rey 1987), and the other, in the fundus of the IAS (Fig. 6, sections f–h, and Fig. 7, sections f and g), to the dysgranular area 44 (Petrides et al. 2005; Belmalih et al. 2009). In all the frontal areas, except for area 12o, the laminar distribution of the labeling showed a typical *intermediate* pattern (Felleman and van Essen 1991) with labeled cells almost equally concentrated in the supragranular versus the

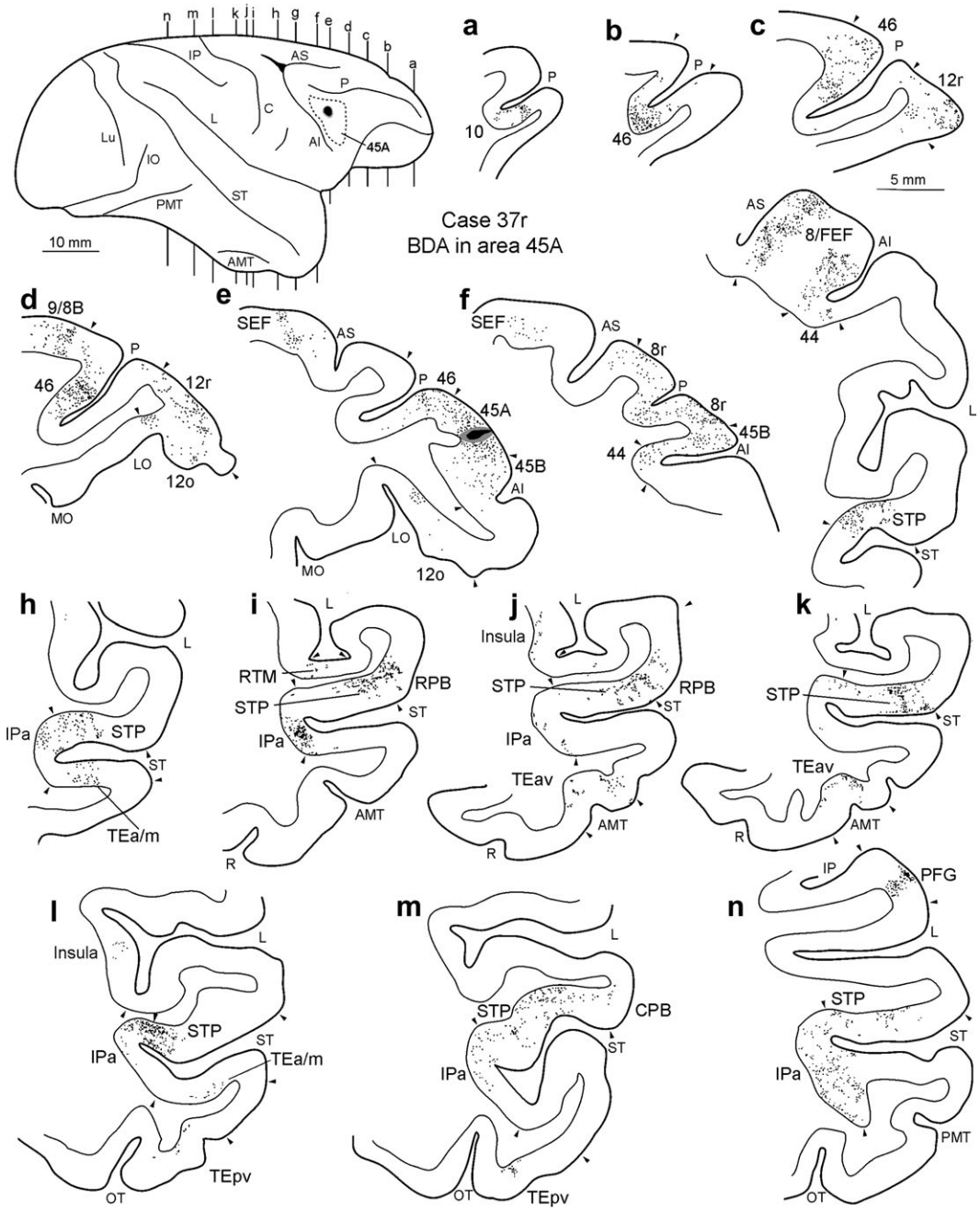

Figure 7. Distribution of the anterograde labeling observed in Case 37r BDA, shown in drawings of coronal sections. Sections are shown in a rostral to caudal order (a–n). The dot density is proportional to the density of the observed labeled terminals. Arrowheads indicate borders between different areas. The dorsolateral view of the injected hemisphere in the upper left part of the figure shows the levels at which the sections were taken, the border of area 45A and the location of the injection site. Abbreviations as in Figures 1 and 5.

infragranular layers (*bilaminar* pattern), and anterograde labeling was almost evenly distributed across all the cortical layers (*columnar* pattern). In area 12o, the labeled cells and terminals were by far denser in layers V–VI and IV–VI, respectively.

Outside the frontal lobe, rich connections were observed with the temporal cortex (Fig. 5), mostly with the STG, where >20% of the labeled cells were observed in both Cases 36l CTBg and 37l FB. Two STG sectors were very densely labeled: 1) the caudal and the rostral parabelt auditory cortex (Kaas and Hackett 2000; Saleem et al. 2008) on the gyral convexity (CPB and RPB, Fig. 6, sections k, l, n, and o, and Fig. 7, sections i, j, and m); and 2) the mid-rostral part of the upper bank of the STS (area STP), where the labeling tended to be aggregated into a more caudal (Fig. 6, sections n and o, and Fig. 7, sections l–n) and a more rostral (Fig. 6, sections k–m, and Fig. 7, sections i–k) zone. In all the cases, weaker labeling was also observed more rostrally in the gyrus (STGr; Kaas and Hackett 2000; Saleem et al. 2008), in the medial auditory belt areas RTM and RM (Fig. 6, sections k and l, Fig. 7, section i) and in the lateral auditory belt area RTL (Fig. 6, section j). Additional labeling in the temporal lobe in Cases 37l and 37r was found in

Table 2

Percent distribution (%) and total number (*n*) of labeled neurons observed following representative tracer injections in areas 45A, 45B, ventral 8/FEF, 8r, ventrocaudal 46, and caudal 12r

Injected area	45A		45B			8/FEF		8r		46		12	
Case	C36l CTBg	C37l FB	C26l DY	C36l FB	C30r FB	C36r FR	C37l CTBg	C37l CTBr	C39r FB	C23l FB	C26l CTBg	C26l FB	C39r DY
VLPF and DLPF													
45A	X	X	18.4	16	21.5	2	2.7	2.1	5.3	1.9	1.5	35.9	39.2
45B	4.1	4.9	X	X	X	13.5	9.9	5.4	8.1	2	2	12.9	6.9
12l	12.3	12	11.6	8	11.9	*	*	*	*	1	1.9	16	10.1
12r, caudal half	5	3.1	12.2	6.3	8.6	1.6	*	–	–	14	6.2	X	X
12r, rostral half	–	*	5.3	3	3.5	–	–	–	–	5	3.6	2.5	8.5
46 ventral	–	*	6.4	10	2.4	2.6	2	13.8	6.8	X	X	7.5	6.5
46 dorsal	6.3	11.7	3	4.2	3	*	–	4.8	7.1	2.3	*	*	1.1
10	5.9	7.9	–	*	–	–	–	–	–	–	–	–	*
9/8B	9.3	7.2	1.9	3.5	1.9	–	–	*	–			–	–
Orbitofrontal													
12o	14.1	9	*	1.5	*	–	–	–	–	*	*	1.1	7.5
13m	–	–	1.7	2	1	–	–	–	–	–	–	1.7	1.3
12m	–	–	1	1.2	*	–	–	*	–	–	–	4.4	5.2
11	–	–	*	*	–	–	–	*	–	*	–	–	*
Prearcuate													
8/FEF	7.4	8.1	18.1	16.1	25.1	X	X	62.2	60.3	*	*	6.7	2.5
8r	*	1.2	9	6	9.8	30.1	27.3	X	X	12.6	7.8	1.7	2.6
Premotor													
SEF	1.1	1.3	1	1.5	*	1.8	4.3	1.4	1	–	–	*	*
44, F5	2.5	5.1	1	1.5	1.2	1.1	*	*	–	32.1	32	*	*
Parietal													
LIP	–	–	1.5	1.5	2	9	19.1	5	7.6	2.5	*	–	–
Opt	–	–	*	1.5	*	–	–	–	–	–	–	–	–
AIP, PG, PFG, PF	*	*	–	–	–	1	2.7	–	–	13	24.5	–	–
Opercular	–	–	–	–	–	–	–	–	–	4.1	15.5	–	–
Temporal													
Auditory belt/parabelt	14.3	8.3	–	–	–	–	–	–	–	–	–	–	*
STP	13	12	–	*	–	2.9	*	*	*	*	–	–	*
IPa, TEa/m, TE, TEO	*	3.1	4.4	8.4	7.3	18.2	13.3	*	*	1.2	*	7.2	4
MT, FST, MST	–	*	–	*	*	4.1	3.7	1.4	1.1	–	–	–	–
V2–V4	–	–	–	–	–	10.8	12.1	1.6	1	–	–	–	–
Insula	*	1.5	*	*	*	–	–	–	–	3.1	1	*	*
Cingulate	2.1	1.2	2	3.8	*	*	*	*	*	*	*	*	*
Others	*	*	*	*	*	*	*	*	*	3.3	3	*	*
Total neurons	3983	15 386	16 483	27 581	23 951	5332	3631	8092	11 929	22 874	6492	9705	14 ;306

Note: X = injected area; * = labeling < 1%; – = no labeling.

the fundal STS area IPa (Fig. 6, section m, and Fig. 7, section i), in the rostralmost parts of area STP and TEa/m (Fig. 6, sections i and j, and Fig. 7, section h), and more sparsely, with different subdivisions of the inferotemporal area TE that was not observed in case 36l. In Case 37r BDA, there was a relatively weak labeling in antero-ventral TE (TEav) and postero-ventral TE (TEpv) also (Fig. 7, sections j–m), where no retrograde label was observed in Case 37l. In all the various connected temporal areas, the labeled cells showed a *bilaminar* distribution pattern. Labeled terminals, though distributed across all the layers, showed different distribution patterns: in the STG areas (Fig. 8*A*) they were dense throughout lower layer III and layers IV–VI, resembling, to some extent, a *columnar* pattern; in area IPa (Fig. 8*B*), they were densest in layers IV and lower layer III, resembling, to some extent, a *feedforward* pattern (Felleman and van Essen 1991); and in rostral TEa/m (Fig. 8*C*), they were much denser in layer I and poor in layer IV, resembling, to some extent, a *feedback* pattern (Felleman and van Essen, 1991).

Finally, in all the cases, a weak, *intermediate* connection was observed with the IPL convexity area PFG (Figs. 5, 6, section o, and Fig. 7, section n). Some clusters of labeled cells or terminals were also observed in the granular insula and the rostral cingulate area 24 mostly in the deep layers.

Connections of Area 45B

Figures 9–11 and Table 2 show the distribution of the retrograde labeling that resulted from retrograde tracers injections in area 45B (Cases 26l DY, 36l FB, and 30r FB) and Figure 12 shows the distribution, in Case 36r, of the BDA-labeled terminals (blue dots; area 45B injection), together with that of the FR-labeled terminals (red dots; area 8/FEF injection), visualized with the double-labeling procedure described in the Methods section (see, e.g., Fig. 12, A and B). Very similar was the distribution of the retro-anterograde labeling observed in Case 37r FR. Altogether, these cases demonstrated a connectivity pattern of area 45B, qualitatively and quantitatively, which was quite consistent across different cases and markedly different from that of area 45A.

In the frontal lobe (Figs. 9, 10, and 12), dense connections were observed with areas 45A, 12l, and the caudal half of area 12r (Fig. 11, sections c–e, and Fig. 12, section b). However, dense labeling was also located very caudally in both dorsal and ventral area 46 and in ventral area 8r (Fig. 11, sections e–g, and Fig. 12, sections b–d), both very poorly connected with area 45A. Furthermore, dense labeling was observed in area 8/FEF, but unlike area 45A, was denser in the ventral part of this area (Fig. 11, section h, and Fig. 12, section e) in all cases, except Case 30r FB. More rostrally, there were dense connections with the rostral part of the ventral area 46 (Fig. 11, section b) and the rostral half of area 12r (12r rostral in Table 2; Fig. 11, section a and, Fig. 12, section a), which were very poorly or not connected at all with area 45A, respectively. In the DLPF, the labeling was mostly restricted to area 8B (Fig. 11, section d, and Fig. 12, section c), and no labeling was observed in areas 10 and

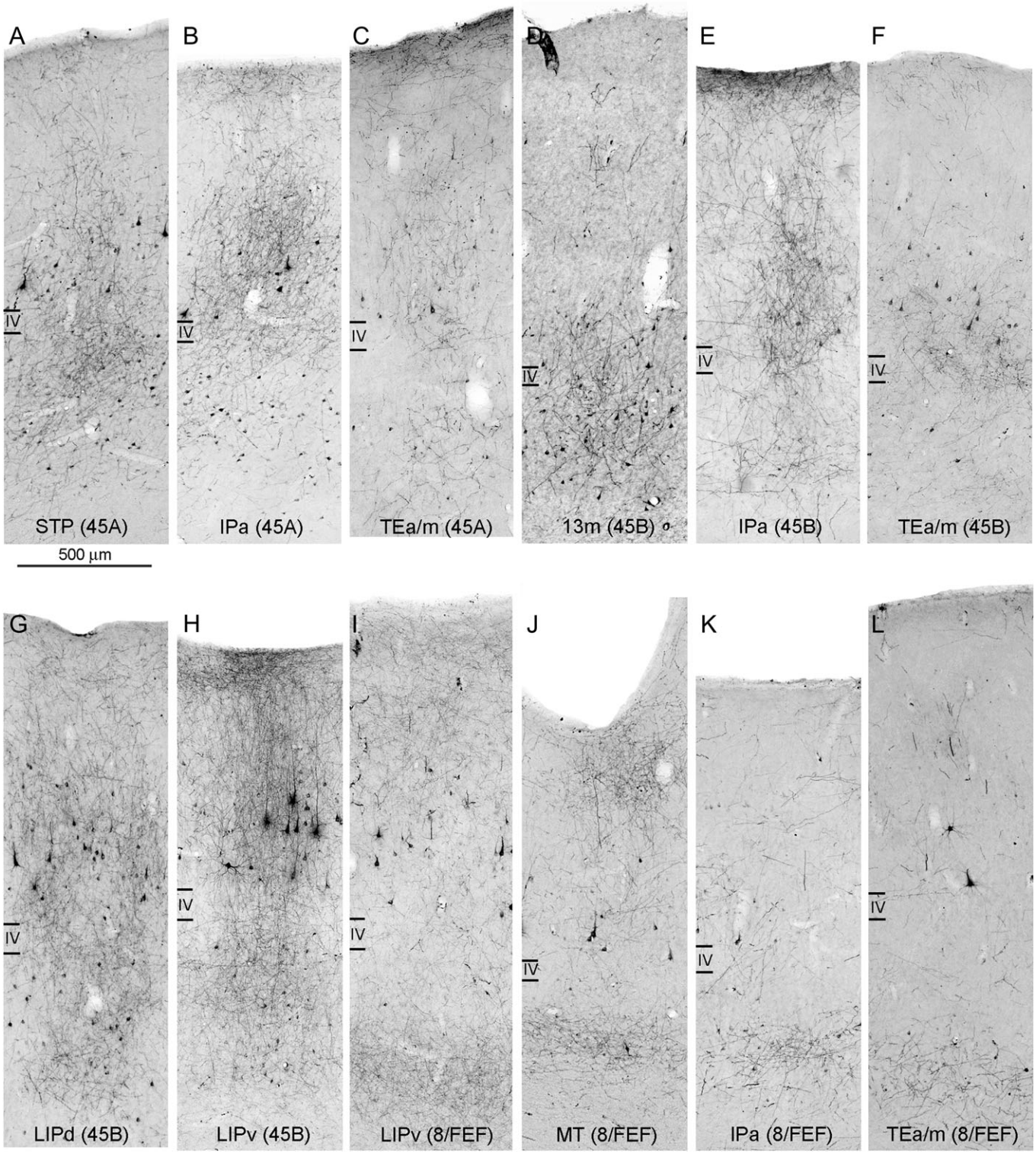

Figure 8. Examples of laminar patterns of retrograde and anterograde labeling observed following injections in areas 45A (*A–C*), 45B (*D–H*), and 8/FEF (*I–L*). In each photomicrographs is indicated the area in which the labeling was observed and, in parentheses, the injected area. (*A–C*) Taken from Case 39l FR, (*D* and *F–H*) from Case 37r FR, (*E*) from Case 36r BDA, and (*I–L*) from Case 36r FR. Calibration bar applies to all photomicrographs.

dorsorostral 46. In the orbitofrontal cortex, with respect to area 45A, the labeling was quantitatively less rich (about 2–3% of labeled cells), but more extensive, involving areas 12m, 13m, and 12o and, less constantly, area 11 (Fig. 11, sections b–e, g and h, and Fig. 12, sections b and c). In area 12o, the labeling avoided its more medial part that, in contrast, was labeled following injections in area 45A. The only significantly labeled frontal sector outside the prefrontal cortex was the SEF (Fig. 11, section e, and Fig. 12, sections d and e). The labeling in area 44 was rather weak (Fig. 11, section g). All these

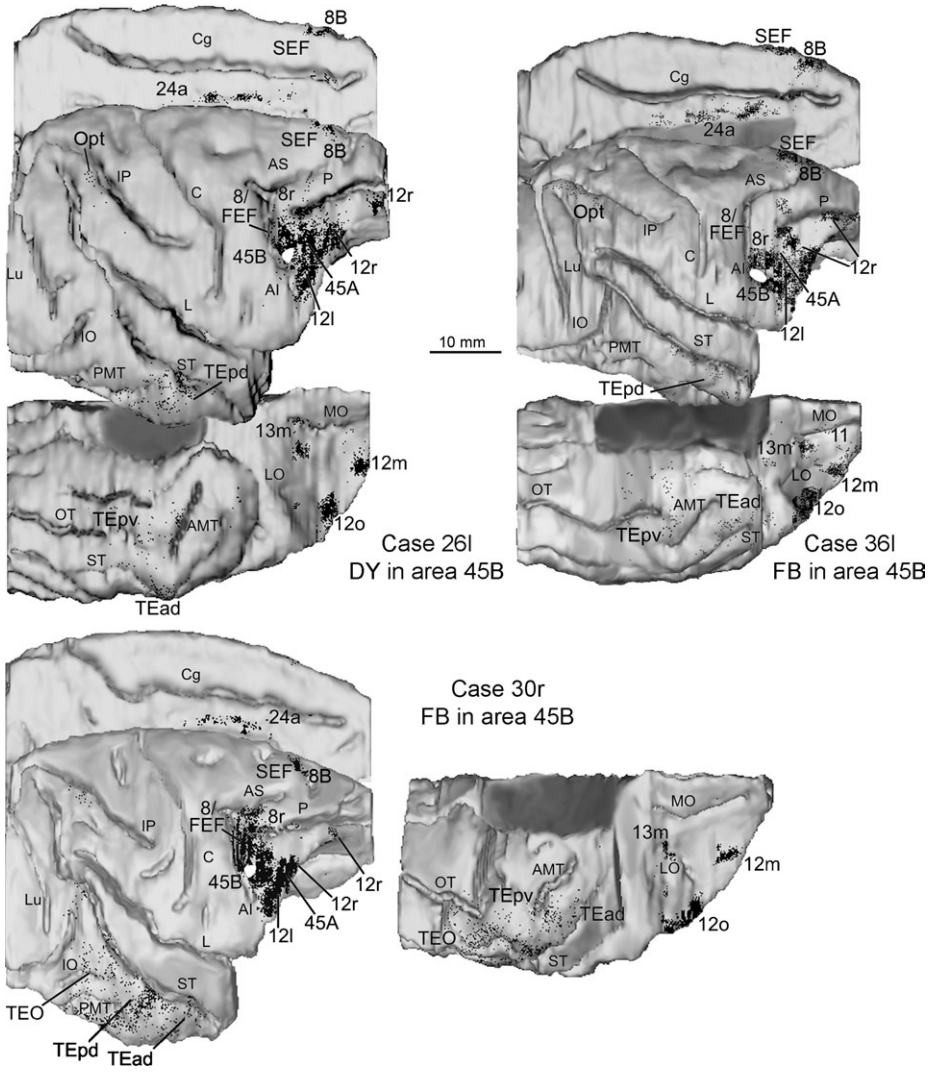

Figure 9. Distribution of the retrograde labeling observed following injections in area 45B in Cases 26l DY, 36l FB, and 30r FB, shown in dorsolateral, mesial and bottom views of the 3D reconstructions of the injected hemispheres. Conventions and abbreviations as in Figures 1 and 5.

connections showed a typical *intermediate* pattern, except for those with orbitofrontal areas, in which the labeled cells and terminals were predominant in the deep layers (Fig. 8D).

Outside the frontal lobe, most of the connections of area 45B were with the temporal cortex (Fig. 9, 10, and 12). These connections, however, were weaker than those of area 45A (about 6% of the labeled cells), and virtually all were confined to the fundus of the STS and inferotemporal cortex. Specifically, the labeling was densest in area TEa/m, at an intermediate rostrocaudal level and in the adjacent part of area IPa (Fig. 11, sections j–l, and Fig. 12, sections g and h). Weaker labeling was located more rostrally in the STS. Additional labeling was consistently observed on the inferotemporal convexity cortex, in different subdivisions of area TE and was denser in posterodorsal TE (TEpd) (Fig. 11, sections j–l, and Fig. 12, sections g and h). In Case 30r FB, sparse labeling extended more caudally, in area TEO. In Cases 36r BDA and 37r FR, a weak connection was observed with area TF. Virtually absent was the labeling in the STG. In areas TEa/m and IPa, where the labeling was densest, the labeled cells had a *bilaminar* distribution pattern. The labeled terminals were densest in layers lower III and IV in area TEa/m (Fig. 8*F*), whereas in area IPa, they were very dense in layer I as well and relatively poor in layer IV (Fig. 8*E*), which is the reverse of that observed for the connections of area 45A with these 2 areas.

Additional, relatively weak connections were observed with the posterior parietal cortex (Figs 9, 10, and, Fig. 12), mostly with the lateral intraparietal area (LIP; Fig. 11, section m, and Fig. 12, section k), where, though with some variability across the cases, the labeling tended to be denser more dorsally, possibly in the dorsal subdivision of LIP (LIPd; Blatt et al. 1990). Here, marked neurons showed a *bilaminar* distribution pattern and labeled terminals were densest throughout the layers lower III–VI, resembling, to some extent, an *intermediate* pattern (Fig. 8*G*). In Case 37r FR, some labeling, located more ventrally, showed a *feedback* pattern with dense labeled terminals in all the layers, except layer IV (Fig. 8*H*). A weak connection was also observed in all the cases with the caudalmost IPL convexity area Opt. Finally, in the rostral cingulate cortex, relatively dense labeled cells and terminals,

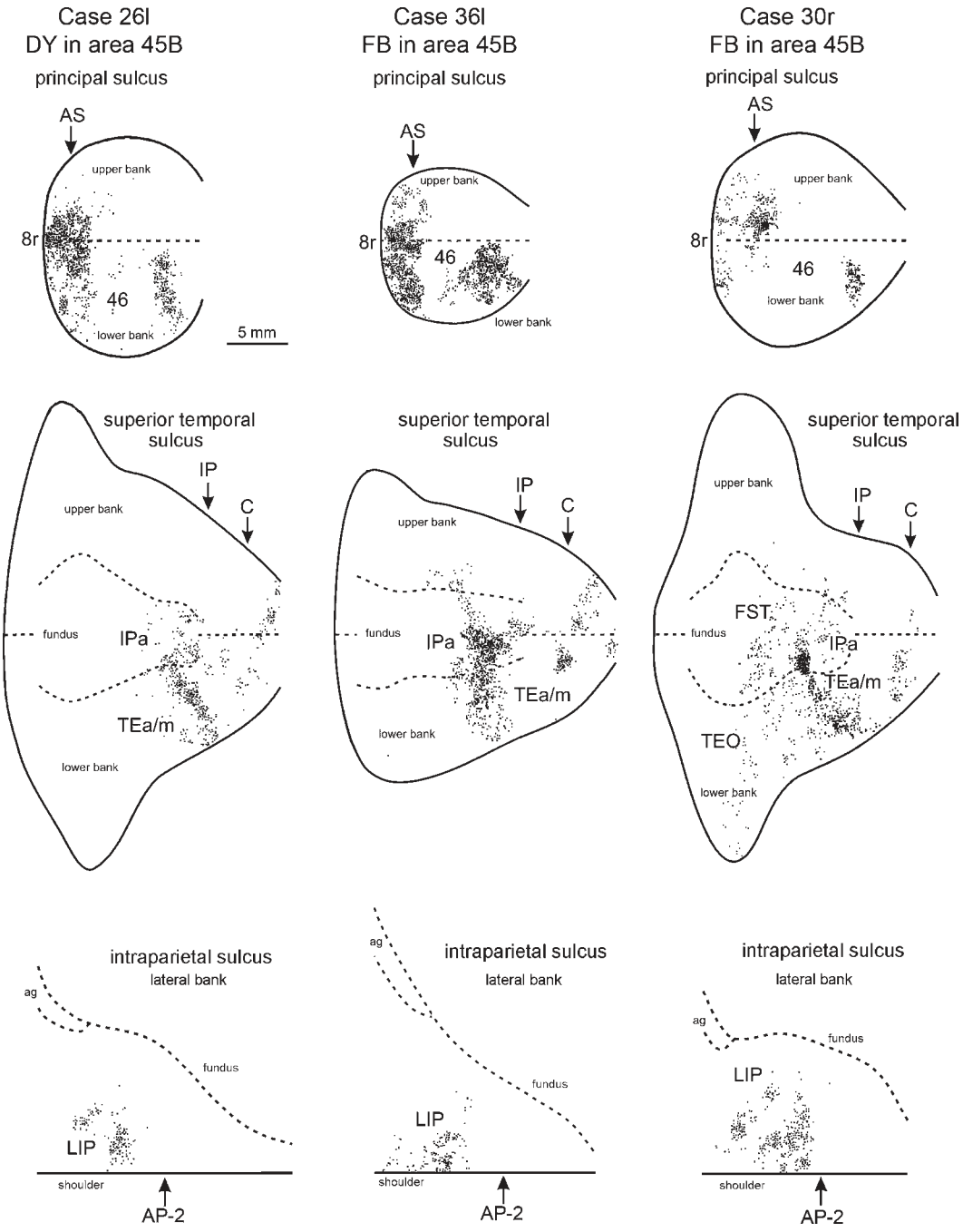

Figure 10. Distribution of the retrograde labeling observed following injections in area 45B in Cases 26l DY, 36l FB, and 30r FB, shown in 2D reconstructions of the PS, the STS and the lateral bank of the IPS. Each 2D reconstruction of the lateral bank of the IPS was aligned to correspond with the lip of the bank, indicated by a continuous line. The dotted line corresponds to the fundus. The arrow marks the antero-posterior stereotaxic level −2, corresponding to the border of area AIP with area LIP (Borra et al., 2008). ag = annectant gyrus. Other conventions and abbreviations as in Figures 1 and 5.

predominant in the deep layers, were observed in different subdivisions of area 24 (Figs 9 and 12).

Connections of Areas 8/FEF and 8r

Connections of Area 8/FEF

The results from Cases 36l DY, 36r FR, and 37l CTBg were in agreement with the data from other studies in which the ventral part of the FEF, where small amplitude saccades are represented (sFEF; Bruce et al. 1985), was injected after physiological identification (Huerta et al. 1987; Stanton et al. 1993; Schall et al. 1995; Stanton et al. 1995). Thus, these data appeared appropriate for comparing the connectivity patterns of area 45B and sFEF, even in the same case (e.g., Case 36r, Fig. 12). Figures 13 and 14 show the distribution of the marked cells found in Cases 36r FR and 37l CTBg. The distribution of the retrograde labeling observed in Case 36l DY was very similar. The percent distribution of the labeling in Cases 36r FR and 37l CTBg is shown in Table 2.

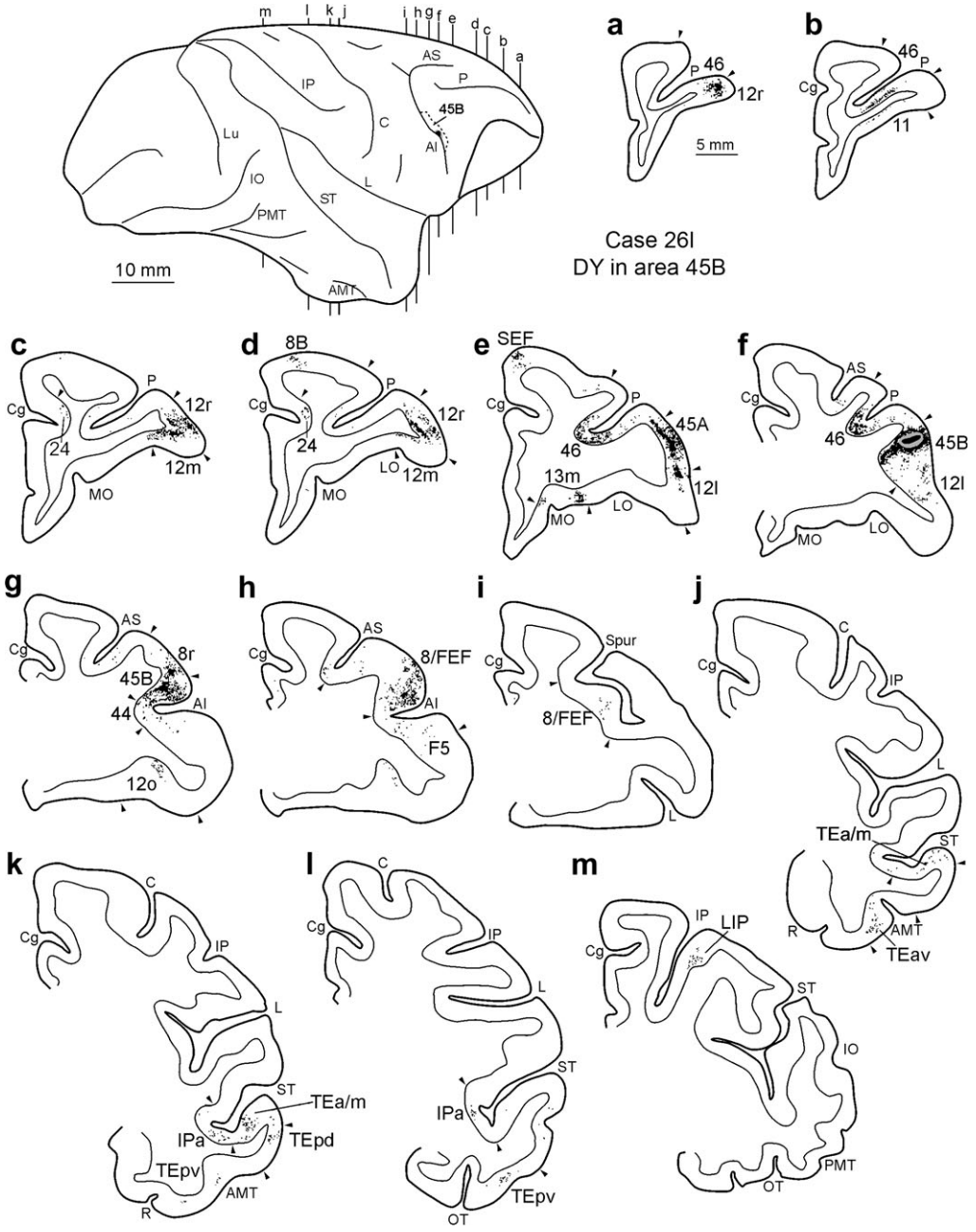

Figure 11. Distribution of the retrograde labeling observed in Case 26l DY, shown in drawings of coronal sections. Sections are shown in a rostral to caudal order (a–m). The dorsolateral view of the injected hemisphere in the upper left part of the figure shows the levels at which the sections were taken, the border of area 45B and the location of the injection site. Conventions and abbreviations as in Figures 1, 5, and 6.

In the prefrontal cortex (Figs 12 and 13), the connections of ventral area 8/FEF were much more limited and weaker than those of area 45B (about 45 vs. 85%, respectively), exclusively involving only areas 8r and 45B densely (Fig. 12, section d, and Fig. 14, sections d, and e), and areas 45A and caudalmost 12r, less densely (Fig. 12, section b and c, and Fig. 14, sections a–c). Except for a few labeled terminals observed in Case 36r in areas 8B and caudal 46, any other prefrontal area was labeled. Dense labeling was also observed corresponding to the SEF, largely overlapping the territory connected with area 45B (Fig. 12, sections d and e, and Fig. 14, section e). Finally, labeling was observed caudal to area 8/FEF (Fig. 12, section f, and Fig. 14, section g), possibly in the smooth-pursuit eye movements field (Stanton et al. 2005). All these connections showed an *intermediate* pattern.

Extensive connections were observed with several areas of the STS and inferotemporal convexity cortex (Figs 12 and 13). In the STS, there were connections with areas TEa/m, IPa, and TEO (Fig. 12, sections g–j, and Fig. 14, sections h–j), and the labeling in area STP was almost negligible. In area TEa/m, the labeling was denser in its intermediate part, that is, in the part of the area densely connected with area 45B also. However, in Cases 36r and 36l, in which tracers were placed in both the areas ventral 8/FEF and 45B, the densest labeling in area TEa/m derived from area 8/FEF injections tended to be located slightly more caudally than that derived from area 45B injections (see, e.g., Fig. 12, 2D

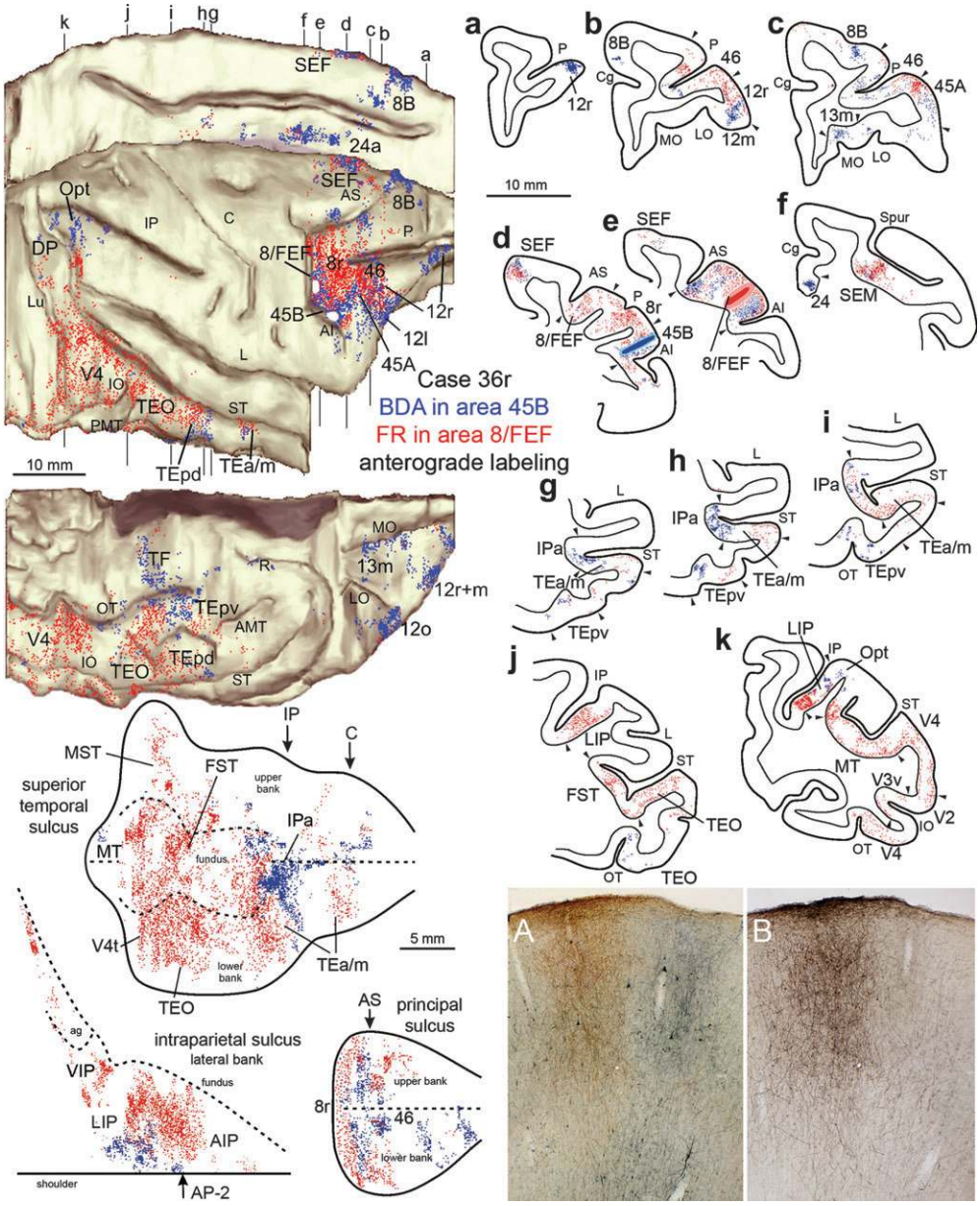

Figure 12. Distribution of the anterograde labeling observed following injections in areas 45B (BDA injection, blue dots) and ventral 8/FEF (FR injection, red dots) in Case 36r, shown in a dorsolateral, a mesial and a bottom view of the 3D reconstruction of the injected hemisphere (upper left), in 2D reconstructions of the STS, the lateral bank of the IPS, and the PS (lower left) and in drawings of coronal sections arranged in a rostral to caudal order (a–k; right). The levels at which the sections were taken are indicated in the dorsolateral and the mesial view of the injected hemisphere. Conventions and abbreviations as in Figures 1, 5, 7, and 10. In the lower right part of the figure, photomicrographs taken in correspondence of the SEF, show, in (*A*), an example of the BDA (stained in brown) and the FR (stained in blue) labeling, visualized with the double-labeling protocol and, in B, the BDA labeling visualized in the adjacent section with the standard protocol.

reconstruction of the STS). More caudally in the STS, there were moderate connections with the fundal superior temporal (FST) and the middle temporal (MT) areas (Fig. 12, sections j and k, and Fig. 14, sections j and k), and very sparse labeled cells were located in the medial superior temporal area (MST). On the inferotemporal convexity cortex, a relatively sparse labeling involved mostly areas TEpd and TEO (Figs 12 and 13). In all the cases, a relatively high proportion of the labeling (about 11–12% of the labeled cells) was observed in area V4 and V4t, but also, more sparsely, in the visual extrastriate areas V3d, V3v, V3a, and V2 (Fig. 12, section k, and Fig. 14, sections l–n). All these connections showed a typical, or almost typical, *feedback* pattern. In all the cases, the marked cells were located by far predominantly in layer III (*supragranular* pattern). The FR-labeled terminals in Case 36r were densest in layers I and VI in areas TEO, caudal STS areas, and visual extrastriate areas (Fig. 8*J*), and were mostly concentrated in layer VI in areas IPa, TEa/m, and TE (Fig. 8*K,L*). This last pattern was markedly different from that observed in areas IPa and TEa/m following injections in areas 45B and 45A.

In the posterior parietal cortex, dense connections were observed with LIP (Fig. 12, sections j and k, and Fig. 14, sections j and k) and the anterior intraparietal (AIP) area (Fig. 14, section i). In LIP, the labeling tended to be located more ventrally with respect to that observed for area 45B (see, e.g., Fig. 12, 2D reconstruction of the IPS), possibly involving mostly

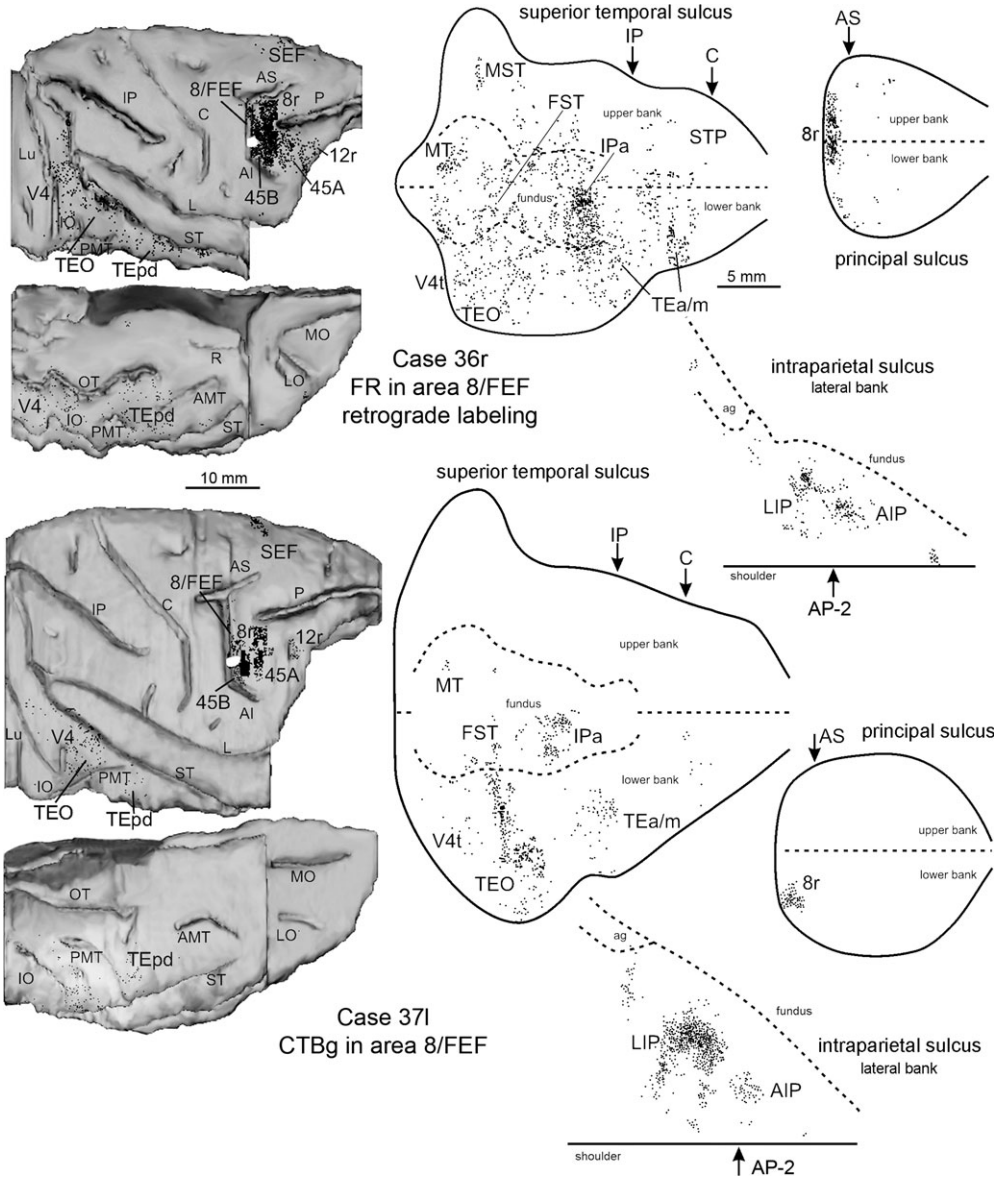

Figure 13. Distribution of the retrograde labeling observed following injections in ventral area 8/FEF in Cases 36r FR and 37l CTBg, shown in dorsolateral and bottom views of the 3D reconstructions of the injected hemispheres (left) and in 2D reconstructions of the lateral bank of the IPS, the PS and the STS (right). Conventions and abbreviations as in Figures 1, 5, and 10.

the ventral subdivision of LIP (LIPv; Blatt et al. 1990). In both AIP and LIP, the marked neurons showed a *supragranular* pattern and the labeled terminals were densest in layers I, II, and upper III, and VI (*feedback* pattern; Fig. 8I). Finally, weak labeling was observed in the cingulate areas 24a (Fig. 14, section g) and 24c.

Case 35r FR (Fig. 15) showed a markedly different connectivity pattern: the labeling was very dense not only in areas 8r, 45B, and the SEF, but also in areas 45A, caudalmost 46, 8B, and rostrally in dorsal 46. All these connections showed an *intermediate* pattern. Furthermore, in the temporal cortex, there were weak *feedback* connections with the inferotemporal areas and area IPa and dense *feedback* connections with areas STP and MST, auditory parabelt areas (mostly CPB), and more caudally, area Tpt. Further labeling was observed in the location of the medial auditory belt area MM. Moderate connections were observed with the visual extrastriate areas V2, V3, V4, and V4t, as well as MT and the dorsal aspect of the prelunate gyrus (area DP, Andersen et al. 1990). In the posterior parietal cortex, the labeling densely involved areas AIP and LIP (both LIPd and LIPv) and, on the mesial surface of the hemisphere, area PGm and the caudal part of the cingulate gyrus (posterior cingulate cortex, CGp; Olson et al. 1996). Finally, dense labeling was observed in areas 24c, 24a, and 23a. Comparison with other studies focused on the FEF connectivity (Huerta et al. 1987; Stanton et al. 1993; Schall et al. 1995; Stanton et al. 1995), clearly suggested that, in this case, the injection site involved not only the sFEF, but also, possibly even more, the FEF sector where larger amplitude saccades are represented (lFEF; Bruce et al. 1985).

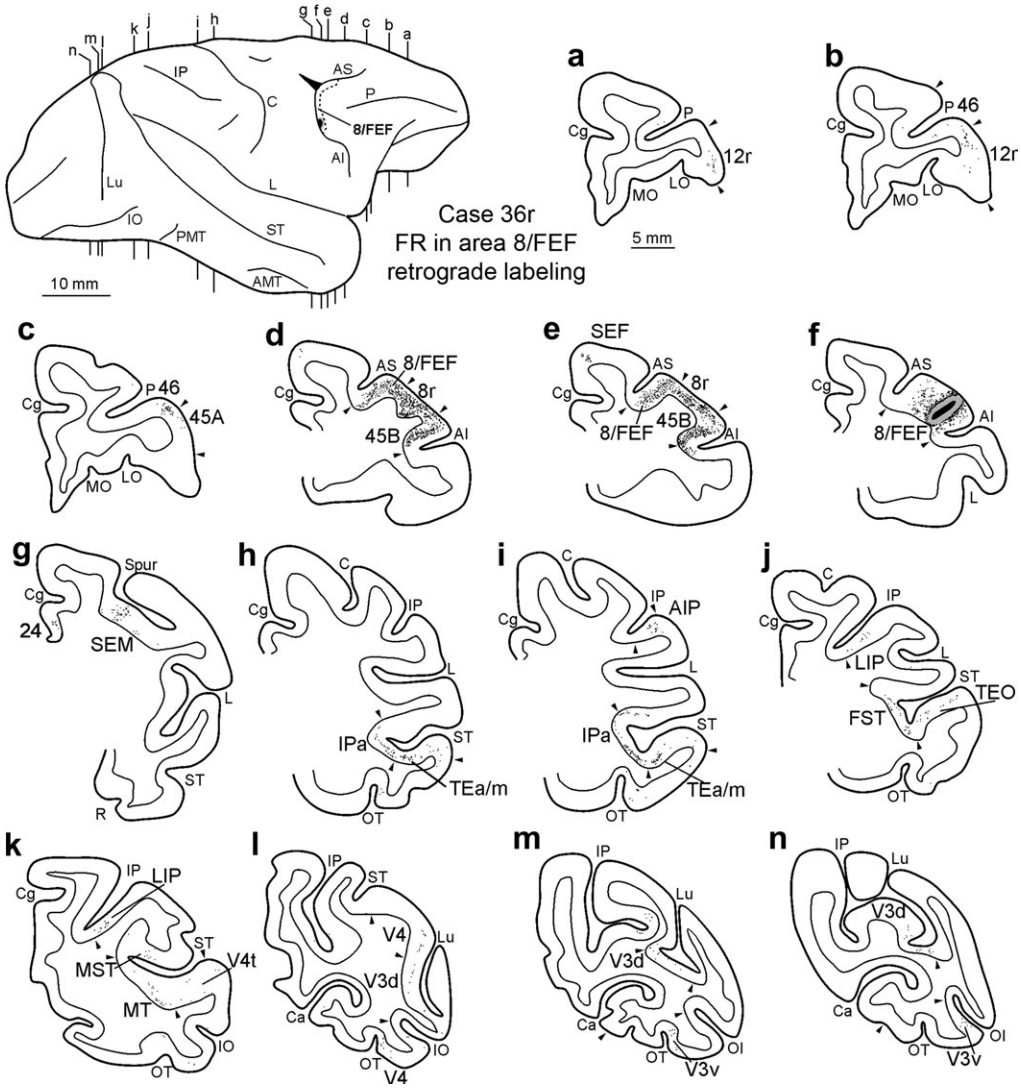

Figure 14. Distribution of the retrograde labeling observed in Case 36r FR, shown in drawings of coronal sections. Sections are shown in a rostral to caudal order (a–n). The dorsolateral view of the injected hemisphere in the upper left part of the figure shows the levels at which the sections were taken, the border of area 8/FEF and the location of the injection site. Conventions and abbreviations as in Figures 1, 5, and 6.

Connections of Area 8r

The results from Cases 39r FB and 37l CTBr showed that area 8r, or at least its mid-ventral part, displays a connectivity pattern clearly different from the adjacent areas 8/FEF, 45B and 45A. Figure 16 shows the distribution of the retrograde labeling observed in Case 39r FB and that observed in the lateral bank of the IPS in Case 37l CTBr, for the sake of comparison with Case 37l CTBg (area 8/FEF injection). The percent distribution of the labeling observed in the 2 cases is shown in Table 2. The frontal connectivity of area 8r was similar to, but quantitatively much higher than that of ventral area 8/FEF, involving, in addition to area 8/FEF, the SEF, areas 45B, 45A, and, more weakly, caudalmost area 46 (Fig. 16, sections a–d). Outside the frontal cortex, the only significant connection of area 8r was with area LIP (about 5–7% of the labeled cells), where the labeling tended to form 2 aggregates, located at different dorsoventral levels, possibly involving both LIPd and LIPv (Fig. 16, sections e–g). In the temporal cortex, sparse marked cells were observed in areas FST, MT, V4t, and V4 (Fig. 16, sections e–g).

Connections of Ventrocaudal Area 46 and Caudal Area 12r

Connections of Ventrocaudal Area 46

The results from Cases 23l FB and 26l CTBg were, in general, very similar and can be described based on the distribution of the retrograde labeling observed in Case 23l FB (Fig. 17). The percent distribution of the labeling observed in the 2 cases is shown in Table 2. The observed connectivity pattern was in substantial agreement with other reports based on similar injection sites (Barbas 1988; Petrides and Pandya 2002), and clearly distinguished this area 46 sector from all the other caudal VLPF areas investigated in our study. In the prefrontal cortex, all the marked cells were virtually confined to the VLPF, especially to its more rostral part. Specifically, in both the cases, very dense retrograde labeling extended from the injected sector rostrally, in the ventral area 46 and in the entire rostrocaudal extent of area 12r (Fig. 17, sections a and b), and caudally, in area 8r (Fig. 17, section d). Except for a marginal

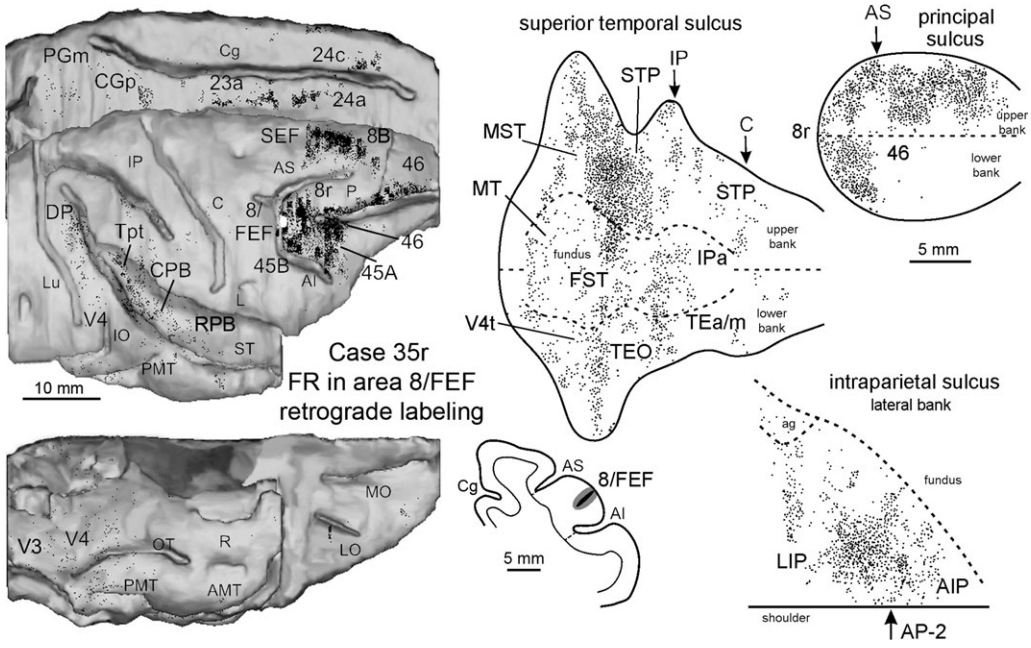

Figure 15. Distribution of the retrograde labeling observed following an injection of FR in a relatively dorsal part of area 8/FEF in Case 35r, shown in a dorsolateral, a mesial and a bottom view of the 3D reconstruction of the injected hemispheres (left) and in 2D reconstructions of the lateral bank of the IPS, of the PS and of the STS (right). Conventions and abbreviations as in Figures 1, 5, and 10.

involvement of the dorsal part of area 45A and few labeled cells in area 12l in Case 23l FB, all the other caudal VLPF areas were devoid of significant labeling. A very high proportion of the retrograde labeling was observed in the dysgranular and agranular frontal cortex (about 31% of the labeled cells). Most of it was located in the rostral ventral premotor area F5, especially in its ventral part, and in area 44 (Fig. 17, sections d–g). A moderate connection was also observed with the mesial agranular frontal area F6 (pre-SMA; Fig. 17, sections d and e). Labeling was also observed in the frontal operculum, in the location of area PrCO. Although only few clusters of marked neurons were observed in areas TEa/m and IPa in the temporal cortex (Fig. 17, g and h), very dense retrograde labeling was observed in the posterior parietal cortex, all virtually confined to the rostral part of the IPL and parietal operculum. In Case 23l FB (more caudal injection), the marked cells were much denser in areas PF, PFG, and AIP, and weaker in area PG and the parietal opercular areas, SII and PV (Fig. 17, sections h–k). In Case 26l CTBg (more rostral injection), the retrograde labeling was densest in the SII/PV region, dense in areas PFG and AIP, weak in area PG, and almost absent in area PF. Finally, dense labeling was observed in the granular insula (Fig. 17, section g). In spite of these differences between the 2 cases, these data clearly indicated that the ventrocaudal part of area 46, adjacent to area 45A, is a major target of rostral areas of the IPL and the parietal operculum.

Connections of Caudal Area 12r

The 2 injections placed in the caudal part of area 12r yielded very similar results, with some quantitative differences attributable to the differences in the size and/or cortical laminar involvement of the injection sites. Given their caudal location in area 12r, these data could only partially describe the connectivity pattern of this area, which extends rostrally as far as area 10 of the frontal pole. However, in the context of our study, these injections were very helpful in showing that the architectonic border between areas 45A and 12r clearly distinguishes 2 connectionally and markedly different prefrontal fields. The results of these 2 cases are shown in Figures 18 and 19, and the percent distribution of the observed labeling is shown in Table 2. In the frontal cortex (Fig. 18), the retrograde labeling was very dense in almost the entire extent of area 12r, in ventral area 46, mostly in its rostral part, and in areas 45A, 45B, and 12l (Fig. 19, sections a–f). Weaker retrograde labeling was also observed in ventral area 8/FEF (Fig. 19, section g), area 8r (Fig. 19, section f), and the SEF (Fig. 19, section d). Furthermore, rich retrograde labeling was observed in the orbitofrontal cortex, mostly in the location of areas 12m, 12o, and 13m (Fig. 19, sections b, d, and f). The only significantly labeled sector outside the frontal lobe was the inferotemporal cortex, where the labeling was mostly concentrated in the rostral and intermediate part of area TEa/m, in area IPa, and in areas TEad and TEpd (Fig. 19, sections h–l).

Discussion

The present study showed that the 2 caudal VLPF architectonic areas 45A and 45B display connectivity patterns that markedly distinguish them from one another and from their neighboring architectonic areas 8/FEF, 8r, 46, and 12r. These data support the distinctiveness of the architectonic areas 45A and 45B, and appear helpful in clarifying some controversial issues about the role of different parts of the caudal VLPF in nonspatial information processing.

Cortical Connectivity of Areas 45A and 45B

Areas 45A and 45B markedly differ in their frontal, temporal, and parietal connectivity (Fig. 20). In the frontal lobe, area 45A displays primary reciprocal connections with the adjacent

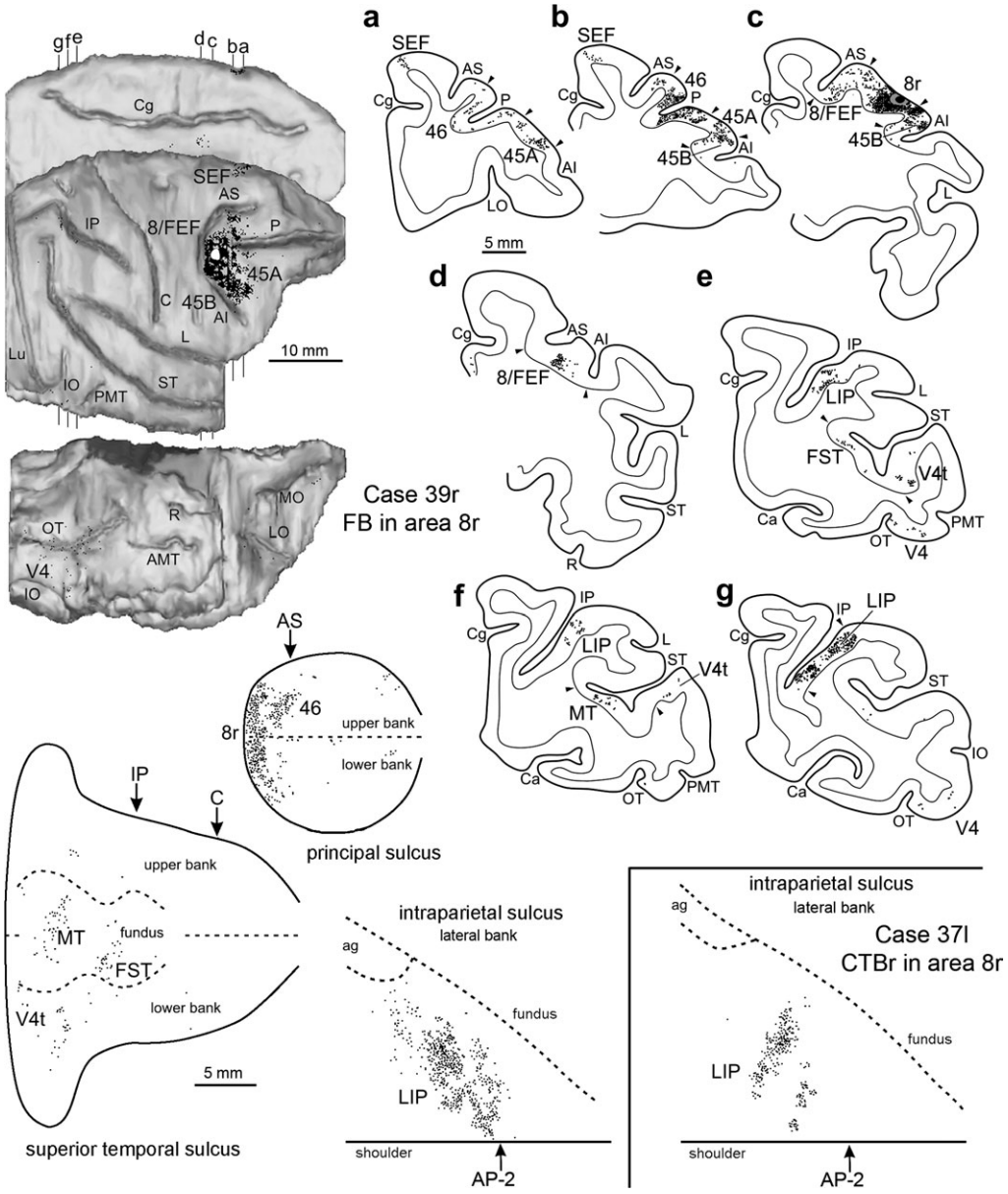

Figure 16. Distribution of the retrograde labeling observed following an injection of FB in area 8r in Case 39r shown in a dorsolateral, a mesial and a bottom view of the 3D reconstruction of the injected hemisphere (upper left), in 2D reconstructions of the STS, of the lateral bank of the IPS and of the PS (lower left) and in drawings of coronal sections arranged in a rostral to caudal order (a–g; right). The levels at which the sections were taken are indicated in the dorsolateral and mesial views of the injected hemisphere. The lower right part of the figure shows the distribution of the retrograde labeling observed in Case 37l CTBr in the lateral bank of the IPS. Conventions and abbreviations as in Figures 1, 5, and 10.

areas 12l and caudal 12r, areas 10, dorsorostral 46 and 9/8B, and orbitofrontal area 12o. Other frontal connections densely involve areas 8/FEF (mostly dorsally) and 44, weakly involve the SEF, and very weakly involve area 8r. Area 45B displays dense reciprocal connections with areas 12l and caudal 12r, but, unlike area 45A, is densely connected with the rostral area 12r and ventrorostral and caudal area 46, weakly connected with area 9/8B (mostly area 8B), and not connected with areas 10 and dorsorostral 46. Orbitofrontal connections are weaker, but more extensive than those of area 45A, involving area 12o, and also areas 13m, 12m, and 11. Connections with areas 8r and 8/FEF (mostly ventrally) are much stronger, those with area 44 are weaker, and those with the SEF are equally dense. In the temporal cortex, area 45A, and not area 45B, displays dense, reciprocal connections with area STP and auditory-related STG areas. Furthermore, though both areas 45A and 45B display reciprocal connections with area IPa and inferotemporal convexity areas, those with area TEa/m involve largely segregated parts of this area and are by far denser for area 45B. In the parietal cortex, minor reciprocal connections with areas LIP and Opt distinguish area 45B from area 45A, which has only a weak connection with area PFG.

The present data largely extend the results of the only earlier study focused on the connectivity of area 45 (Petrides and Pandya 2002), in which relatively large tracer injections placed close or corresponding to the shoulder of the IAS, failed to distinguish between the connections of areas 45A and 45B. The results of Petrides and Pandya (2002) appear fully compatible with an involvement of both these areas with respect to their tracer injections.

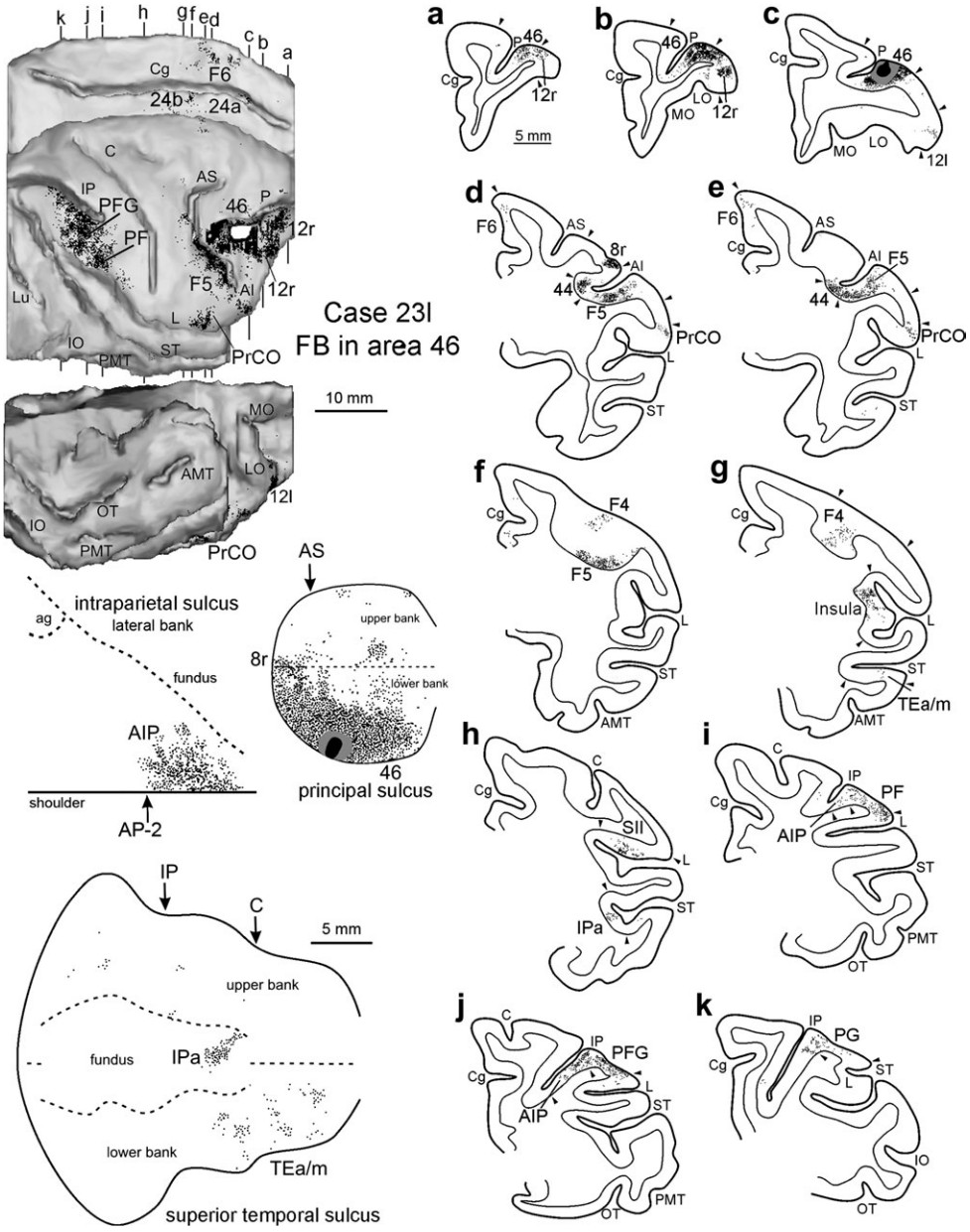

Figure 17. Distribution of the retrograde labeling observed following an injection of FB in ventrocaudal area 46 in Case 23I, shown in a dorsolateral, a mesial and a bottom view of the 3D reconstruction of the injected hemisphere (upper left), in 2D reconstructions of the PS, of the lateral bank of the IPS and of the STS (lower left) and in drawings of coronal sections arranged in a rostral to caudal order (a–k; right). The levels at which the sections were taken are indicated in the dorsolateral and mesial views of the injected hemisphere. Conventions and abbreviations as in Figures 1, 5, and 10.

Furthermore, some available indirect evidence is in line with the present data. First, the prefrontal connectivity of area 45A, and not area 45B, with areas 10 and dorsorostral 46, and the much stronger connectivity of area 45A with the DLPF convexity cortex, is confirmed by tracer injections in areas 10 (Petrides and Pandya 2007), 9, and dorsorostral 46 (Petrides and Pandya 1999), showing labeling in the location of area 45A, and not area 45B. Second, the connectivity of area 45A, and not area 45B, with the STG is confirmed by tracer injections in the location of area STP (Seltzer and Pandya 1989; Saleem et al. 2008) or in the lateral parabelt or belt auditory areas (Petrides and Pandya 1988; Hackett et al. 1999; Romanski, Tian, et al. 1999; Saleem et al. 2008; Munoz et al. 2009) showing VLPF connections limited to the location of area 45A. In contrast, as expected from our data, injections in areas TE and TEa/m yielded labeling in the location of both areas 45A and 45B (Shiwa 1987; Seltzer and Pandya 1989; Webster et al. 1994; Saleem et al. 2008). However, the connections of area TEa/m (Seltzer and Pandya 1989; Saleem et al. 2008) with area 45A were more extensive when tracers were placed more rostrally in area TEa/m, as expected from our observation that the intermediate area TEa/m almost selectively projects to area 45B. Finally, in line with our data, labeling in the ventralmost part of the prearcuate bank (area 45B) was observed following tracer injections in LIP (Cavada and Goldman-Rakic 1989; Lewis and Van Essen 2000) or Opt (Rozzi et al. 2006). A connection of the middle of the IPL convexity cortex with area 45A was observed following a large tracer injection by Cavada and Goldman-Rakic (1989), and by Rozzi et al. (2006; see their

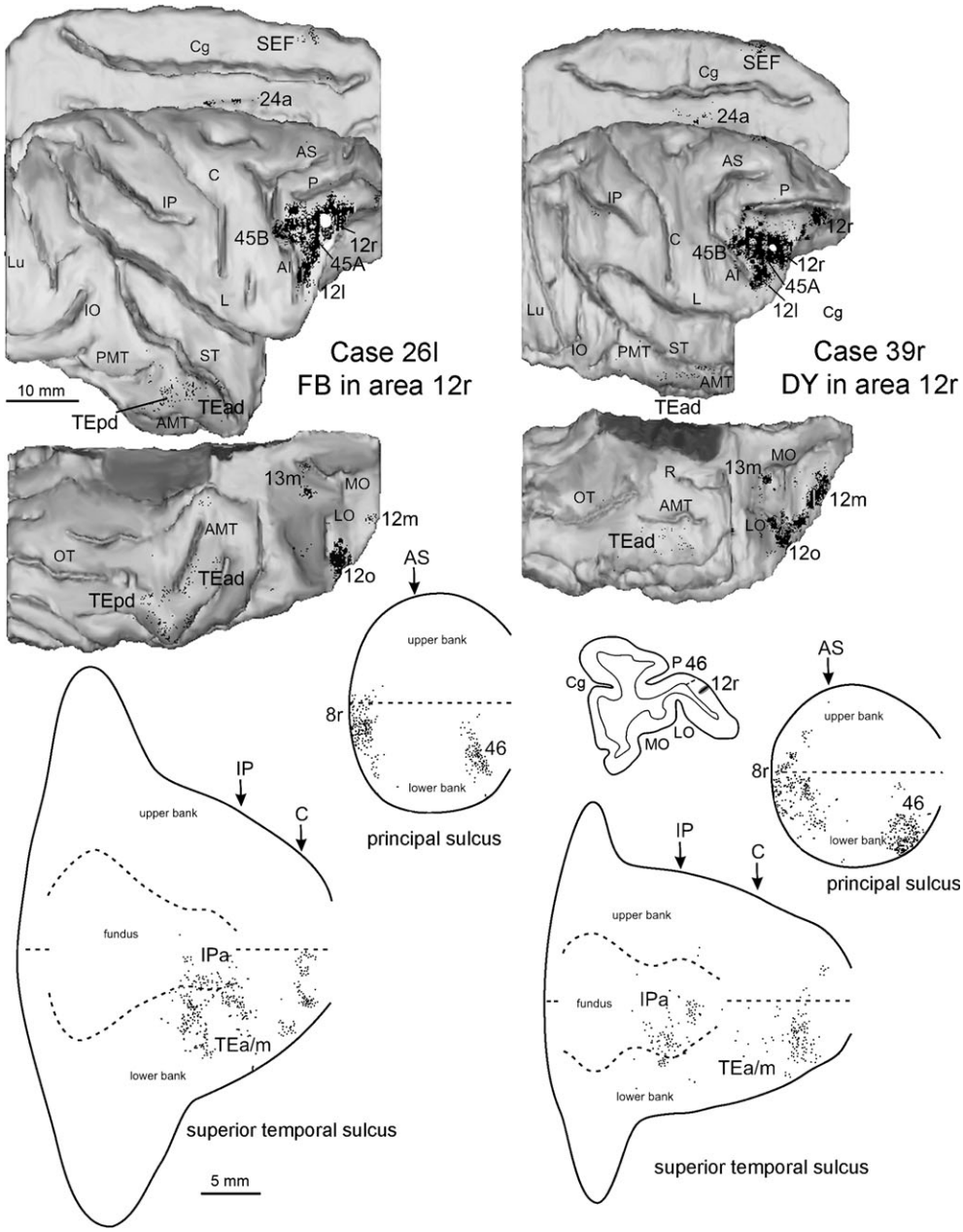

Figure 18. Distribution of the retrograde labeling observed following injections in caudal area 12r in Cases 26l (FB) and 39r (DY), shown in dorsolateral, mesial and bottom views of the 3D reconstructions of the injected hemispheres (upper part) and in 2D reconstructions of the PS and of the STS (lower part). Conventions and abbreviations as in Figures 1 and 5.

Fig. 12), who observed a very weak connection following injections in area PFG.

Laminar Distribution of Areas 45A and 45B Connections

Differences in the laminar origin and termination of the cortical connections have been used as an indicator of the direction of information flow and hierarchical organization within the sensory systems (e.g., Rockland and Pandya 1979; Maunsell and Van Essen 1983; Felleman and Van Essen 1991). According to Felleman and Van Essen (1991), these differences can be brought back to 3 main qualitatively different patterns: *feed-forward* connections, linking lower-order with higher-order areas; *feedback* connections, linking higher-order with lower-order areas; and *intermediate* connections, linking areas located at the same hierarchical level.

In our study we found that, in several cases, the connections of areas 45A and 45B could not be easily fit in this model, as already noted by Webster et al. (1994), for the prefrontal connectivity of areas TE and TEO. However, according to Barbas et al. (Barbas 1986; Barbas and Rempel-Clower 1997; Barbas et al. 2002; Medalla and Barbas 2006), the connections of frontal areas show laminar patterns that differ much more quantitatively rather than qualitatively, depending on the degree of structural differences (e.g., laminar differentiation, cell density) between the connected areas. Indeed, the laminar

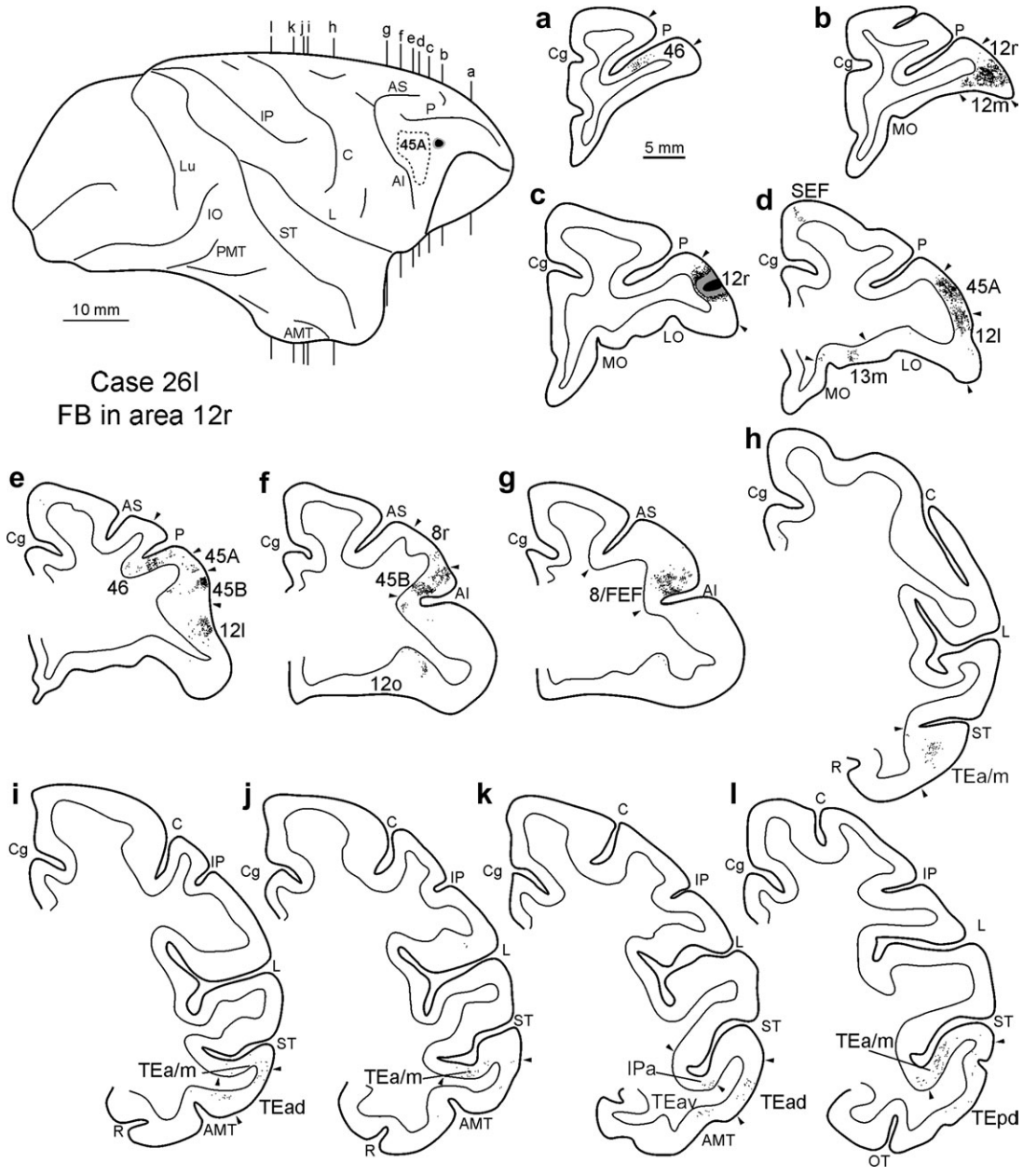

Figure 19. Distribution of the retrograde labeling observed in Case 26l FB, shown in drawings of coronal sections. Sections are shown in a rostral to caudal order (a–l). The dorsolateral view of the injected hemisphere in the upper left part of the figure shows the levels at which the sections were taken, the border of area 45A and the location of the injection site. Conventions and abbreviations as in Figures 1 and 5.

pattern of the orbitofrontal connections of areas 45A and 45B (i.e., labeled cells and terminals mostly in the deep layers) is exactly similar to that described by Barbas et al. (2002) for the connections of more differentiated VLPF areas with less differentiated orbitofrontal areas. In this view, the laminar patterns of the primary temporal connections of area 45A with STG areas and area IPa, and of area 45B with area TEa/m, densest in layers III–VI or in lower layer III and layer IV, are those expected for the prefronto-temporal connections linking areas of similar structure (Rempel-Clower and Barbas 2000).

In a general sense, the differences in the laminar patterns of connections may subtend the differences in the functional interaction between the connected areas (Barbas 2002). In this regard, it must be noted that the projections from areas 45A and 45B to area IPa, the only nonfrontal area where we observed a significant overlap of their connections, showed quite different laminar connection patterns.

Distinctiveness of Areas 45A and 45B with Respect to their Neighboring Areas

A further important objective of our study was to assess whether connectivity patterns distinguish: 1) area 45B from areas 8/FEF and 8r; and 2) area 45A from areas 46 and 12r.

Our data from the ventral area 8/FEF injections were fully congruent with other connectional studies focused on the sFEF (Huerta et al. 1987; Stanton et al. 1993; Schall et al. 1995; Stanton et al. 1995), and showed a connectivity pattern markedly

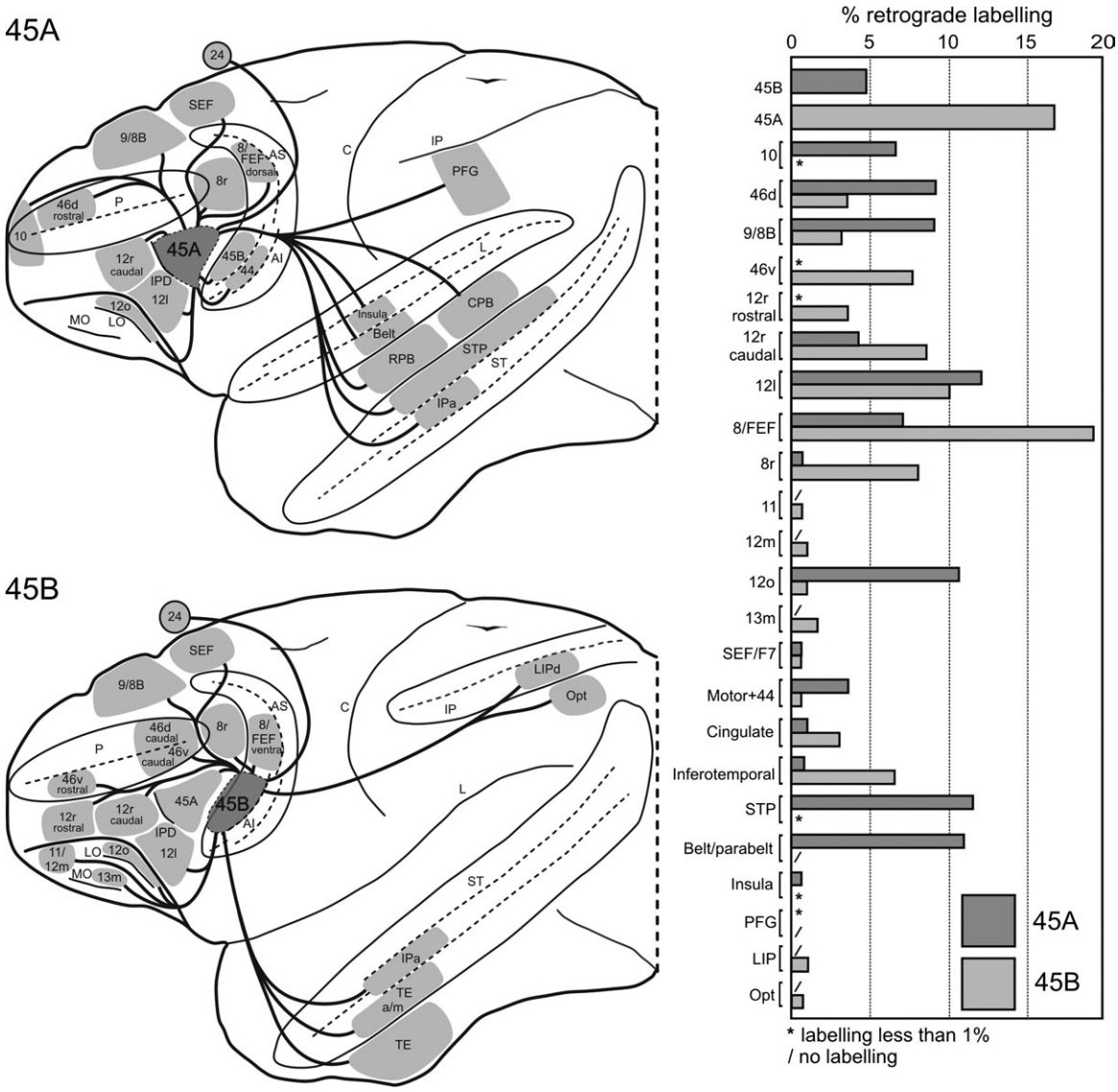

Figure 20. Summary view of the major ipsilateral cortical connections of areas 45A and 45B and mean percent distribution of the retrograde labeling observed in the cases of injections in areas 45A and 45B listed in Table 2. Abbreviations as in Figures 1 and 5.

different from that of area 45B. First, we observed that the prefrontal connections of ventral area 8/FEF were limited to the neighboring caudal VLPF areas, and were much weaker (45% of the labeled cells) than those of areas 45B (85%) and 8r (88%). Second, the ventral area 8/FEF displayed consistent *feedback* connections with the caudal temporal (caudal TEa/m, FST, MST, and TEO) and visual extrastriate areas, V2, V3, V4, V4t, and V5/MT, all of them virtually not connected with area 45B. Third, in the IPS, the ventral area 8/FEF, and not area 45B, was observed to be connected with AIP, as already noted in an earlier study (Borra et al. 2008), and the connections of areas 45B and ventral 8/FEF with LIP involved largely segregated sectors of this area. This last finding cannot be simply accounted for by a topographic organization of the prearcuate connectivity of LIP, considering that the connections of areas 45B and 8/FEF with LIP showed different laminar patterns of connections. Finally, in areas IPa, intermediate TEa/m, and TE, which are connected with both areas 8/FEF and 45B, the laminar pattern of the area 8/FEF connections showed a supragranular pattern of retrograde labeling and labeled terminals mostly in layer VI. This particular type of *feedback* pattern, also described by Stanton (1995), is markedly different from that of area 45B, suggesting a differential functional interaction of areas 8/FEF and 45B with these inferotemporal areas. Accordingly, the present data provide very strong evidence for the distinctiveness of areas 8/FEF and 45B, previously suggested by architectonic (Stanton et al. 1989; Petrides and Pandya 1994, 2002; Gerbella et al. 2007), and functional (Stanton et al. 1989) data.

Area 8r is an architectonic area located just rostral to the FEF (Gerbella et al., 2007), basically corresponding to myeloarchitectonic area 8Ar defined by Preuss and Goldman-Rakic (1991). This area has a very high prefrontal connectivity (88% of the labeled cells), and unlike the adjacent areas 8/FEF, 45B, and 45A, possesses quite a low temporal connectivity, limited to areas MT, FST, and V4. The only robust extrafrontal connection is with the dorsal and the ventral part of LIP. This is in agreement with the data from the study by Medalla and Barbas (2006), showing that although the prearcuate bank

(possibly area 8/FEF) is mostly connected with LIPv, the prearcuate convexity cortex (possibly area 8r) is connected with both LIPv and LIPd. Accordingly, though based on only 2 tracer injections, our data suggest that area 8r represents a further distinct prearcuate subdivision.

Area 46 is a large, architectonically and connectionally nonhomogeneous region (Barbas and Mesulam 1985; Barbas and Pandya 1989; Preuss and Goldman-Rakic 1991; Petrides and Pandya 1994, 1999, 2002). In our study, we focused on the ventrocaudal part of area 46, adjacent to area 45A. In agreement with other previous studies with similar injections (Barbas 1988; Petrides and Pandya 2002), we found that some major connectional features of this area 46 sector were 1) the very strong parietal and premotor connectivity, mostly with rostral IPL and opercular parietal areas and the ventral premotor area F5, respectively; and 2) the very low, if not negligible, temporal connectivity. Thus, in the light of the present study, it is worth mentioning that the architectonic border between areas 46 and 45A marks a sharp connectional border between a parietal-recipient (area 46) and a temporal-recipient (area 45A) prefrontal territory.

Lastly, an important aspect of our study was to assess the possible connectional validity of the architectonic border between areas 45A and 12r, observed at the level of the IPD by Petrides and Pandya (1994, 2002) and Gerbella et al. (2007), more caudally by others (e.g., Preuss and Goldman-Rakic 1991; Romanski, Bates, et al. 1999), or more rostrally (Carmichael and Price 1994).

Our data, in full agreement with those of Petrides and Pandya (2002), indicate that the temporal connectivity of caudal area 12r, all virtually limited to the rostral inferotemporal areas, is a major connectional feature that clearly distinguish this area from area 45A. Romanski, Bates, et al. (1999) found labeling in parabelt auditory areas from large injection attributed to the convexity and orbital parts of area 12. The location of the injection site and the very little, if any, projections from the auditory parabelt to the cortical sector ventral to area 45A (Petrides and Pandya 2002; Saleem et al. 2008) suggest that this labeling possibly resulted from an involvement of area 45A through the injection site. Thus, the present study strongly suggests that area 45A is the architectonic counterpart of the caudal VLPF territory connected with auditory-related areas of the STG.

Functional Considerations

Recent data showed that a restricted VLPF field, located within and just caudal to the IPD, is activated by the observation of faces in monkey functional magnetic resonance imaging (fMRI) experiments (prefrontal lateral, face-sensitive field; Tsao et al. 2008), and hosts neurons responsive to auditory, visual, or combined auditory and visual communication stimuli (Romanski and Goldman-Rakic 2002; Romanski et al. 2005; Sugihara et al. 2006). For this field, Romanski (2004, 2007) suggested a role in the control of communication behavior, based on integration of inputs from STG auditory-related areas and the higher-order multisensory area STP (Bruce et al. 1981). According to Romanski (2004, 2007), this field is located in the caudal part of area 12, where a rostral STG-recipient territory, mostly corresponding to area 12, overlaps a caudal inferotemporal-recipient territory that mostly corresponds to area 45. However, a different view was proposed by Petrides and Pandya (2002; see also Petrides 2005): area 45 is the caudal VLPF STG- and STP-recipient territory, whereas area 12 (12/47 in the terminology of these authors) is a more rostral inferotemporal-recipient VLPF territory. Our data appear helpful in solving this discrepancy, suggesting that area 45A represents the architectonic counterpart of this caudal VLPF STG- and STP-recipient territory.

Additional evidence suggests a broader role of area 45A in the visual and audiovisual processing, possibly related to communication behavior. First, monkey fMRI experiments showed that this area is activated by the observation of actions made by others (Nelissen et al. 2005), an aspect of visual information of behavioral relevance in animals with a complex social life, such as primates. The connections with area STP, hosting visual neurons coding different types of biological motions (see, e.g., Oram and Perrett 1994; Barraclough et al. 2005) and activated by observation of actions in monkey fMRI experiments (Nelissen et al. 2006), represent the possible pathway mediating this specific aspect of visual processing. Furthermore, area 45A is connected with a dorsal prearcuate territory involving the lFEF, but is also likely to be connected with a field containing auditory-responsive neurons and associated with pinna and eye movements (Burman et al. 1988; Azuma and Suzuki 1984; Schall et al. 1995). Finally, the frontal connections of area 45A involve dorsal area 8/FEF, the SEF, dorsorostral area 46, and area 12o. In turn, the dorsal area 8/FEF (Huerta et al. 1987; Stanton et al. 1993; Schall et al. 1995; Stanton et al. 1995; present data), the SEF (Huerta and Kaas 1990; Luppino et al. 2001, 2003; Wang et al. 2005), and the dorsorostral area 46 (Seltzer and Pandya 1989; Petrides and Pandya 1999; Saleem et al. 2007) are connected to each other, and as area 12o (Carmichael and Price 1995; Saleem et al. 2007) are connected to STG auditory-related areas and STP. Thus, area 45A is involved in a superior temporal–frontal network, possibly representing the neural substrate of the role of gaze position and eye movements, with respect to communication behavior. In fact, in area STP there are face or body-parts responsive neurons sensitive to the gaze direction, which may be relevant in understanding where the conspecifics are focused (see, e.g., Carey et al. 1997). Furthermore, behavioral studies showed that 1) in monkeys, eye-gaze direction is important in the expression of dominant or submissive social signaling (Tate et al. 2006); and 2) when viewing vocalizing conspecifics, monkeys focus predominantly on the eye region of the agent, and this strategy might be useful to glean information about his/her intentions (Ghazanfar et al. 2006).

Our data also indicate that area 45B is a distinct inferotemporal-recipient caudal VLPF area. A major connectional feature of this area is the strong linkage with areas ventral 8/FEF and 8r. Indeed, area 45B possibly corresponds to the ventral prearcuate field tightly connected with the FEF, designated as FV by Huerta et al. (1987). Furthermore, 2-deoxyglucose data have shown that the prearcuate sector activated by the execution of saccadic eye movements extends ventrally to the FEF, in the location of area 45B (Moschovakis et al. 2004). These data, therefore, suggest an affiliation of area 45B to the oculomotor frontal system. However, intracortical microstimulation of this area is not effective in evoking eye movements with low-threshold currents (e.g., Bruce et al. 1985; Stanton et al. 1989), suggesting that this area is less directly connected with the extraocular motor neurons, than the FEF. Furthermore, unlike areas 8/FEF and 8r, area 45B is connected with the rostral prefrontal and orbitofrontal areas and lacks connections

with areas located at relatively earlier stages of visual information processing. Thus, area 45B might have a unique role in the frontal oculomotor system, representing the gateway for the access of highly integrated information from the rostral prefrontal areas and motivational information from the orbitofrontal areas to the control of eye movements. Finally, area 45B displays a laminar connection pattern with the inferotemporal areas different from that of area 8/FEF, which could subtend differences in the functional interaction of these 2 areas with the ventral visual stream areas.

To our knowledge, no one has directly investigated the physiological properties of this area. However, monkey fMRI experiments have shown that area 45B, and not the FEF, is activated by the observation of actions and shapes (Nelissen et al. 2005) or faces (prefrontal arcuate, face-sensitive field; Tsao et al. 2008), which can be explained by the connections with area TEa/m, involved in visual coding of object-oriented actions (Perrett et al. 1989), faces (Tsao et al. 2006), and 3D shapes (Janssen et al. 2001). Future studies may clarify the possible functional role of this area in nonspatial information processing, and whether this area indeed plays a role in the control of eye movements. Based on these data, one possible working hypothesis is that area 45B is a "preoculomotor" area, where rostral prefrontal, orbitofrontal, and inferotemporal inputs guide the exploration of visual scenes for the perception of actions, objects, and faces.

Conclusions

The present data indicate that at least for the caudal VLPF, the notion of a prefrontal cortex fractionated into sectors specified by different connectivity patterns, initially put forward by Goldman-Rakic (1987), is valid even at the level of individual architectonic areas. This notion, however, does not imply that each prefrontal area acts as an independent unit. The rich intraprefrontal connectivity observed for areas 45A and 45B may certainly represent the neural substrate for the proposed role of the prefrontal cortex in higher-order integrative processes (see, e.g., Miller et al. 2002; Tanji and Hoshi 2008). Our data indicate that intraprefrontal connections (see, e.g., the frontal connectivity of area 45A) may be rather specific and organized in networks of interconnected frontal areas, sharing common connections with the posterior associative areas, as originally proposed by Carmichael and Price (1996; see also Saleem et al. 2008). The exact definition of these networks is a possible key for gaining new insights on the regional functional specialization and the integrative processes of the prefrontal cortex, and certainly is a challenge for the future anatomical studies.

Funding

Ministero dell'Università e della Ricerca (grant number: PRIN 2006, n° 2006052343_002); Belgian Science Policy Office (grant number: IUAP P6/29); European Union Marie Curie Early stage training program "Sensoprim" (grant number: MEST-CT-2004-007825) to A.B.

Notes

The 3D reconstruction software was developed by CRS4, Pula, Cagliari, Italy. *Conflict of Interest*: None declared.

Address correspondence to Professor Giuseppe Luppino, Dipartimento di Neuroscienze, Sezione di Fisiologia, Università di Parma, Via Volturno 39, I-43100 Parma, Italy. Email: luppino@unipr.it.

References

Andersen RA, Asanuma C, Essick G, Siegel RM. 1990. Corticocortical connections of anatomically and physiologically defined subdivisions within the inferior parietal lobule. J Comp Neurol. 296: 65–113.

Azuma M, Suzuki H. 1984. Properties and distribution of auditory neurons in the dorsolateral prefrontal cortex of the alert monkey. Brain Res. 298:343–346.

Barbas H. 1986. Pattern in the laminar origin of corticocortical connections. J Comp Neurol. 252:415–422.

Barbas H. 1988. Anatomic organization of basoventral and mediodorsal visual recipient prefrontal regions in the rhesus monkey. J Comp Neurol. 276:313–342.

Barbas H, Ghashghaei HT, Rempel-Clower N, Xiao D. 2002. Anatomic basis of functional specialization in prefrontal cortices in primates. In: Grafman J, editor. Handbook of neuropsychology. Amsterdam: Elsevier Science. p. 1–27.

Barbas H, Mesulam MM. 1985. Cortical afferent input to the principalis region of the rhesus monkey. Neuroscience. 15:619–637.

Barbas H, Pandya DN. 1989. Architecture and intrinsic connections of the prefrontal cortex in the rhesus monkey. J Comp Neurol. 286:353–375.

Barbas H, Rempel-Clower N. 1997. Cortical structure predicts the pattern of corticocortical connections. Cereb Cortex. 7:635–646.

Barraclough NE, Xiao D, Baker CI, Oram MW, Perrett DI. 2005. Integration of visual and auditory information by superior temporal sulcus by neurons responsive to the sight of actions. J Cogn Neurosci. 17:377–391.

Belmalih A, Borra E, Contini M, Gerbella M, Rozzi S, Luppino G. 2009. Multimodal architectonic subdivision of the rostral part (area F5) of the macaque ventral premotor cortex. J Comp Neurol. 512:183–217.

Bettio F, Demelio S, Gobbetti E, Luppino G, Matelli M. 2001. Interactive 3-D reconstruction and visualization of primates cerebral cortex. Soc Neurosci Abstr. 728.724.

Blatt GJ, Andersen RA, Stoner GR. 1990. Visual receptive field organization and cortico-cortical connections of the lateral intraparietal area (area LIP) in the macaque. J Comp Neurol. 299:421–445.

Borra E, Belmalih A, Calzavara R, Gerbella M, Murata A, Rozzi S, Luppino G. 2008. Cortical connections of the macaque anterior intraparietal (AIP) area. Cereb Cortex. 18:1094–1111.

Boussaoud D, Ungerleider L, Desimone R. 1990. Pathways for motion analysis: cortical connections of the medial superior temporal and fundus of the superior temporal visual areas in the macaque. J Comp Neurol. 296:462–495.

Bruce C, Desimone R, Gross CG. 1981. Visual properties of neurons in a polysensory area in superior temporal sulcus of the macaque. J Neurophysiol. 46:369–384.

Bruce CJ, Goldberg ME, Bushnell C, Stanton GB. 1985. Primate frontal eye fields. II. Physiological and anatomical correlates of electrically evoked movements. J Neurophysiol. 54:714–734.

Burman D, Bruce CJ, Russo GS. 1988. Pinna movements elicited by microstimulation in the prefrontal cortex of monkeys. Soc Neurosci Abstr. 14:208.

Carey DP, Perrett DI, Oram MW. 1997. Recognizing, understanding and reproducing actions. In: Boller F, Grafman J, editors. Handbook of neuropsychology. Amsterdam: Elsevier. p. 111–129.

Carmichael ST, Price JL. 1994. Architectonic subdivision of the orbital and medial prefrontal cortex in the macaque monkey. J Comp Neurol. 346:366–402.

Carmichael ST, Price JL. 1995. Sensory and premotor connections of the orbital and medial prefrontal cortex of macaque monkeys. J Comp Neurol. 363:642–664.

Carmichael ST, Price JL. 1996. Connectional networks within the orbital and medial prefrontal cortex of macaque monkeys. J Comp Neurol. 371:179–207.

Cavada C, Goldman-Rakic PS. 1989. Posterior parietal cortex in rhesus monkey: II. Evidence for segregated corticocortical networks linking sensory and limbic areas with the frontal lobe. J Comp Neurol. 287:422–445.

Felleman DJ, Van Essen DC. 1991. Distributed hierarchical processing in primate cerebral cortex. Cereb Cortex. 1:1–47.

Gerbella M, Belmalih A, Borra E, Rozzi S, Luppino G. 2007. Multimodal architectonic subdivision of the caudal ventrolateral prefrontal cortex of the macaque monkey. Brain Struct Funct. 212:269–301.
Ghazanfar AA, Nielsen K, Logothetis NK. 2006. Eye movements of monkey observers viewing vocalizing conspecifics. Cognition. 101:515.
Goldman-Rakic P. 1987. Circuitry of primate prefrontal cortex and regulation of behavior by representational memory. In: Plum F, Mountcastle F, editors. Handbook of physiology. Washington (DC): The American Physiological Society. p. 373–515.
Gregoriou GG, Borra E, Matelli M, Luppino G. 2006. Architectonic organization of the inferior parietal convexity of the macaque monkey. J Comp Neurol. 496:422–451.
Hackett TA, Stepniewska I, Kaas JH. 1999. Prefrontal connections of the parabelt auditory cortex in macaque monkeys. Brain Res. 817:45–58.
Huerta MF, Kaas JH. 1990. Supplementary eye field as defined by intracortical microstimulation: connections in Macaques. J Comp Neurol. 293:299–330.
Huerta MF, Krubitzer LA, Kaas JH. 1987. Frontal eye field as defined by intracortical microstimulation in squirrel monkeys, owl monkeys, and macaque monkeys II. Cortical connections. J Comp Neurol. 265:332–361.
Janssen P, Vogels R, Liu Y, Orban GA. 2001. Macaque inferior temporal neurons are selective for three-dimensional boundaries and surfaces. J Neurosci. 21:9419–9429.
Kaas JH, Hackett TA. 2000. Subdivisions of auditory cortex and processing streams in primates. Proc Natl Acad Sci USA. 97:11793–11799.
Levy R, Goldman-Rakic PS. 2000. Segregation of working memory functions within the dorsolateral prefrontal cortex. Exp Brain Res. 133: 23–32.
Lewis JW, Van Essen DC. 2000. Corticocortical connections of visual, sensorimotor, and multimodal processing areas in the parietal lobe of the macaque monkey. J Comp Neurol. 428:112–137.
Luppino G, Belmalih A, Borra E, Gerbella M, Rozzi S. 2008. Cortical connections of the macaque areas 45A and 45B and of their neighboring caudal ventrolateral prefrontal areas. 2008 Program No 387.23. Neuroscience Meeting Planner. Washington (DC): Society for Neuroscience.
Luppino G, Calzavara R, Rozzi S, Matelli M. 2001. Projections from the superior temporal sulcus to the agranular frontal cortex in the macaque. Eur J Neurosci. 14:1035–1040.
Luppino G, Rozzi S, Calzavara R, Matelli M. 2003. Prefrontal and agranular cingulate projections to the dorsal premotor areas F2 and F7 in the macaque monkey. Eur J Neurosci. 17:559–578.
Matelli M, Govoni P, Galletti C, Kutz DF, Luppino G. 1998. Superior area 6 afferents from the superior parietal lobule in the macaque monkey. J Comp Neurol. 402:327–352.
Maunsell JHR, Van Essen DC. 1983. The connections of the middle temporal visual area (MT) and their relationship to a cortical hierarchy in the macaque monkey. J Neurosci. 3:2563–2586.
Medalla M, Barbas H. 2006. Diversity of laminar connections linking periarcuate and lateral intraparietal areas depends on cortical structure. Eur J Neurosci. 23:161–179.
Miller EK, Freedman DJ, Wallis JD. 2002. The prefrontal cortex: categories, concepts and cognition. Philos Trans R Soc Lond B Biol Sci. 357:1123.
Morecraft RJ, Louie JL, Herrick JL, Stilwell-Morecraft KS. 2001. Cortical innervation of the facial nucleus in the non-human primate: a new interpretation of the effects of stroke and related subtotal brain trauma on the muscles of facial expression. Brain. 124:176–208.
Morecraft RJ, McNeal DW, Stilwell-Morecraft KS, Dvanajscak Z, Ge J, Schneider P. 2007. Localization of arm representation in the cerebral peduncle of the non-human primate. J Comp Neurol. 504:149–167.
Moschovakis AK, Gregoriou GG, Ugolini G, Doldan M, Graf W, Guldin W, Hadjidimitrakis K, Savaki HE. 2004. Oculomotor areas of the primate frontal lobes: a transneuronal transfer of rabies virus and [14c]-2-deoxyglucose functional imaging study. J Neurosci. 24:5726–5740.
Munoz M, Mishkin M, Saunders RC. 2009. Resection of the medial temporal lobe disconnects the rostral superior temporal gyrus from some of its projection targets in the frontal lobe and thalamus. Cereb Cortex. Advance Access published January 15, doi:10.1093/cercor/bhn236.
Nelissen K, Luppino G, Vanduffel W, Rizzolatti G, Orban GA. 2005. Observing others: multiple action representation in the frontal lobe. Science. 310:332–336.
Nelissen K, Luppino G, Vanduffel W, Rizzolatti G, Orban GA. 2006. Representation of observed actions in macaque occipitotemporal and parietal cortex. Program No 306.12 2006 Neuroscience meeting planner. Atlanta (GA): Society for Neuroscience.
Olson CR, Musil SY, Goldberg ME. 1996. Single neurons in posterior cingulate cortex of behaving macaque: eye movements signals. J Neurophysiol. 76:3285–3330.
Oram MW, Perrett DI. 1994. Responses of anterior superior temporal polysensory (STPa) neurons to 'biological motion' stimuli. Cogn Neurosci. 6:99–116.
Passingham RE, Toni I, Rushworth MFS. 2000. Specialisation within the prefrontal cortex: the ventral prefrontal cortex and associative learning. Exp Brain Res. 133:103–113.
Perrett DI, Harries MH, Bevan R, Thomas S, Benson PJ, Mistlin AJ, Chitty AJ, Hietanen JK, Ortega JE. 1989. Frameworks of analysis for the neural representation of animate objects and actions. J Exp Biol. 146:87–113.
Petrides M. 2005. Lateral prefrontal cortex: architectonic and functional organization. Philos Trans R Soc Lond B Biol Sci. 360:781.
Petrides M, Pandya DN. 1988. Association fiber pathways to the frontal cortex from the superior temporal region in the rhesus monkey. J Comp Neurol. 273:52–66.
Petrides M, Pandya DN. 1994. Comparative architectonic analysis of the human and the macaque frontal cortex. In: Boller F, Grafman J, editors. Handbook of neuropsychology. Amsterdam: Elsevier. p. 17–58.
Petrides M, Pandya DN. 1999. Dorsolateral prefrontal cortex: comparative cytoarchitectonic analysis in the human and the macaque brain and corticocortical connection patterns. Eur J Neurosci. 11: 1011–1036.
Petrides M, Pandya DN. 2002. Comparative cytoarchitectonic analysis of the human and the macaque ventrolateral prefrontal cortex and corticocortical connection patterns in the monkey. Eur J Neurosci. 16:291–310.
Petrides M, Pandya DN. 2007. Efferent association pathways from the rostral prefrontal cortex in the macaque monkey. J Neurosci. 27:11573–11586.
Preuss TM, Goldman-Rakic PS. 1991. Myelo- and cytoarchitecture of the granular frontal cortex and surrounding regions in the streptisine primate *Galago* and the anthropoid primate *Macaca*. J Comp Neurol. 310:429–474.
Rempel-Clower NL, Barbas H. 2000. The laminar pattern of connections between prefrontal and anterior temporal cortices in the rhesus monkey is related to cortical structure and function. Cereb Cortex. 10:851–865.
Rockland KS, Pandya DN. 1979. Laminar origins and terminations of cortical connections of the occipital lobe in the rhesus monkey. Brain Res. 179:3–20.
Romanski LM. 2004. Domain specificity in the primate prefrontal cortex. Cogn Affect Behav Neurosci. 4:421–429.
Romanski LM. 2007. Representation and integration of auditory and visual stimuli in the primate ventral lateral prefrontal cortex. Cereb Cortex. 17:i61–i69.
Romanski LM, Averbeck BB, Diltz M. 2005. Neural representation of vocalizations in the primate ventrolateral prefrontal cortex. J Neurophysiol. 93:734–747.
Romanski LM, Bates JF, Goldman-Rakic PS. 1999. Auditory belt and parabelt projections to the prefrontal cortex in the rhesus monkey. J Comp Neurol. 403:141–157.
Romanski LM, Goldman-Rakic PS. 2002. An auditory domain in primate prefrontal cortex. Nat Neurosci. 5:15.
Romanski LM, Tian B, Fritz J, Mishkin M, Goldman-Rakic PS, Rauschecker JP. 1999. Dual streams of auditory afferents target multiple domains in the primate prefrontal cortex. Nat Neurosci. 2:1131–1136.
Rozzi S, Calzavara R, Belmalih A, Borra E, Gregoriou GG, Matelli M, Luppino G. 2006. Cortical connections of the inferior parietal cortical convexity of the macaque monkey. Cereb Cortex. 16:1389–1417.
Saleem KS, Kondo K, Price JL. 2008. Complementary circuits connecting the orbital and medial prefrontal networks with the temporal,

insular, and opercular cortex in the macaque monkey. J Comp Neurol. 506:659–693.
Saleem KS, Price JL, Hashikawa T. 2007. Cytoarchitectonic and chemoarchitectonic subdivisions of the perirhinal and parahippocampal cortices in macaque monkeys. J Comp Neurol. 500:973–1006.
Saleem KS, Tanaka K. 1996. Divergent projections from the anterior inferotemporal area TE to the perirhinal and entorhinal cortices in the macaque monkey. J Neurosci. 16:4757–4775.
Schall JD, Morel A, King DJ, Bullier J. 1995. Topography of visual cortex connections with frontal eye field in macaque: convergence and segregation of processing streams. J Neurosci. 15:4464–4487.
Schlag J, Schlag-Rey M. 1987. Evidence for a supplementary eye field. J Neurophysiol. 57:179–200.
Seltzer B, Pandya DN. 1989. Frontal lobe connections of the superior temporal sulcus in the rhesus monkey. J Comp Neurol. 281:97–113.
Shiwa T. 1987. Corticocortical projections to the monkey temporal lobe with particular reference to the visual processing pathways. Arch Ital Biol. 125:139–154.
Stanton GB, Bruce CJ, Goldberg ME. 1993. Topography of projections to the frontal lobe from the macaque frontal eye fields. J Comp Neurol. 330:286–301.
Stanton GB, Bruce CJ, Goldberg ME. 1995. Topography of projections to posterior cortical areas from the macaque frontal eye fields. J Comp Neurol. 353:291–305.
Stanton GB, Deng S-Y, Goldberg ME, McMullen NT. 1989. Cytoarchitectural characteristics of the frontal eye fields in macaque monkeys. J Comp Neurol. 282:415–427.
Stanton GB, Friedman HR, Dias EC, Bruce CJ. 2005. Cortical afferents to the smooth-pursuit region of the macaque monkey's frontal eye field. Exp Brain Res. 165:179.
Stanton GB, Goldberg ME, Bruce CJ. 1988. Frontal eye fields efferents in the macaque monkey: I. Subcortical pathways and topography of striatal and thalamic terminal fields. J Comp Neurol. 271: 473–492.
Sugihara T, Diltz MD, Averbeck BB, Romanski LM. 2006. Integration of auditory and visual communication information in the primate ventrolateral prefrontal cortex. J Neurosci. 26:11138–11147.
Tanji J, Hoshi E. 2008. Role of the lateral prefrontal cortex in executive behavioral control. Physiol Rev. 88:37–57.
Tate AJ, Fischer H, Leigh AE, Kendrick KM. 2006. Behavioural and neurophysiological evidence for face identity and face emotion processing in animals. Philos Trans R Soc Lond B Biol Sci. 361:2155.
Tsao DY, Freiwald WA, Tootell RBH, Livingstone MS. 2006. A cortical region consisting entirely of face-selective cells. Science. 311:670–674.
Tsao DY, Schweers N, Moeller S, Freiwald WA. 2008. Patches of face-selective cortex in the macaque frontal lobe. Nat Neurosci. 11:877.
Walker E. 1940. A cytoarchitectural study of the prefrontal area of the macaque monkey. J Comp Neurol. 98:59–86.
Wang Y, Isoda M, Matsuzaka Y, Shima K, Tanji J. 2005. Prefrontal cortical cells projecting to the supplementary eye field and presupplementary motor area in the monkey. Neurosci Res. 53:1–7.
Webster MJ, Bachevalier J, Ungerleider LG. 1994. Connections of inferior temporal areas TEO and TE with parietal and frontal cortex in macaque monkeys. Cereb Cortex. 4:470–483.